# Pressure-Dependence of Water Dynamics in Concentrated Aqueous Poly(*N*-isopropylacrylamide) Solutions with a Methanol Cosolvent

*Bart-Jan Niebuur[1], Wiebke Lohstroh[2], Chia-Hsin Ko[1], Marie-Sousai Appavou[3], Alfons Schulte[4,*], Christine M. Papadakis[1,*]*

[1]Physik-Department, Fachgebiet Physik weicher Materie, Technische Universität München, James-Franck-Str. 1, 85748 Garching, Germany

[2]Heinz Maier-Leibnitz Zentrum (MLZ), Technische Universität München, Lichtenbergstr. 1, 85748 Garching, Germany

[3]Jülich Centre for Neutron Science (JCNS) at Heinz Maier-Leibnitz Zentrum (MLZ), Forschungszentrum Jülich GmbH, Lichtenbergstr. 1, 85748 Garching, Germany

[4]Department of Physics and College of Optics and Photonics, University of Central Florida, 4111 Libra Drive, Orlando, FL 32816-2385, U.S.A.

KEYWORDS. Polymer solutions, thermoresponsive polymers, co-non-solvency, high pressure, poly(*N*-isopropylacrylamide), quasi-elastic neutron scattering, Raman spectroscopy, water dynamics, hydration water

# for Table of Content use only

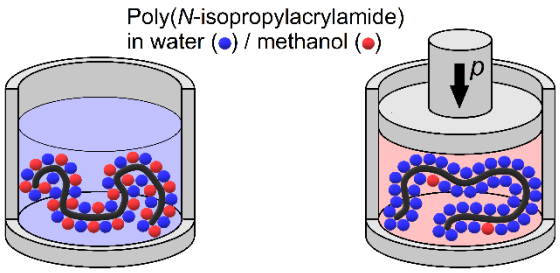


ABSTRACT.

The water dynamics of a concentrated poly(*N*-isopropylacrylamide) (PNIPAM) solution in an 80:20 v/v water/methanol mixture are investigated across the cloud point $T_{cp}$ at atmospheric and high pressure (200 MPa). Quasi-elastic neutron scattering (QENS) reveals the relaxation spectra of bulk and hydration water over a frequency range of four decades (GHz-THz) and their changes upon the reversal of co-non-solvency at high pressure. At atmospheric pressure, the susceptibility spectra in the one-phase region provide evidence of polymer-bound water, which is released in part nearly discontinuously at $T_{cp}$. Simultaneously, the elastic line strength increases abruptly, which is consistent with a coil-to-globule transition. At high pressure, the fraction of bound water decreases gradually with increasing temperature, while the elastic line strength increases at $T_{cp}$. Comparing the bulk diffusion time $\tau_d$ of water in the one-phase region with its values from the neat solvent mixture, dominant methanol adsorption is found at atmospheric pressure, whereas water adsorbs preferentially on the chains at high pressure. At 0.1 MPa, the relaxation time of bound water in the one-phase region near $T_{cp}$ is smaller than at 200 MPa, i.e., the binding strength between water and PNIPAM is weakened by the presence of adsorbed methanol. Raman spectroscopy, probing the interaction between the solvent molecules and the methyl groups of

PNIPAM, indicates that methanol adsorbs to the hydrophobic groups at atmospheric pressure, while it is diminished at high pressure.

## Introduction

Cosolvents are essential in many contexts, including the preparation of pharmaceutical formulations.[1,2] In biological systems, small organic molecules acting as cosolvents can alter the folding/unfolding equilibrium of proteins or facilitate the dissolution of hydrophobic molecules.[3,4] Recently, the effect of a cosolvent on a smart polymer was exploited to isolate single-stranded DNA.[5] In gels and solutions of thermoresponsive polymers, addition of a cosolvent may lead to a strong reduction of the cloud point and reentrant behavior.[6,7,8] These features have been termed co-non-solvency.[9] A prototype responsive polymer in this respect is poly(*N*-isopropylacrylamide) (PNIPAM). At atmospheric pressure, PNIPAM exhibits lower critical solution temperature (LCST) behavior with a cloud point at ~30 °C in purely aqueous solutions,[10] and its solubility is governed by the temperature-dependent hydration of hydrophilic and hydrophobic groups.[10,11] Several water-miscible, organic solvents, e. g. low alcohols, have been shown to lead to co-non-solvency behavior.[12,13,14] Co-non-solvency is significantly altered and even reversed by high pressure.[15,16] In particular, hydration plays a key role for the LCST transition without and with a cosolvent,[17,18,19] yet it has been barely investigated at variable pressure. The molecular mechanisms underlying the pressure-temperature phase diagram have not been fully clarified by experiments. The role of bound and bulk water during phase transitions of PNIPAM in a water/methanol mixture is investigated here by employing quasi-elastic neutron scattering and Raman spectroscopy at variable pressure and temperature.

In the one-phase region at atmospheric pressure, PNIPAM in purely aqueous solution exhibits a coil-like conformation. At $T_{cp}$, cooperative dehydration of the hydrophobic groups sets in[20,21,22] and causes the chains to collapse into compact globules.[23,24] In contrast, the hydrophilic groups remain considerably hydrated above $T_{cp}$.[18,20,21] Thus, upon heating through $T_{cp}$, the overall fraction of hydration water decreases abruptly,[25,26,27] and the mobility of the remaining hydration water is strongly reduced with respect to the one-phase region.[26,27,28,29] In PNIPAM solutions with methanol as a cosolvent, experimental evidence for polymer bound water has come from QENS[30] and dielectric measurements.[31]

As the microscopic origin of co-non-solvency, models based on solvent–cosolvent interactions, cooperative polymer–solvent and polymer–cosolvent hydrogen bonding, and preferential polymer–cosolvent binding have been put forward.[9] Some models suggest that the cosolvent is preferentially bound to the chains.[32,33,34] It tends to colocalize with the hydrophobic isopropyl groups, whereas water interacts preferentially with the hydrophilic amide moieties.[35,36] A recent molecular dynamics investigation found that, at $T_{cp}$, only water is released from the chain, but not the cosolvent (methanol), which alters the chemical potential of water in the bulk mixture.[36] Other theories point to the importance of the solvent-solvent interactions:[37,38] Complexes formed by water and methanol act as a poor solvent for the chains, and thus, solvent-solvent interactions are more preferable than polymer-solvent interactions. A recent neutron structural study combined with molecular dynamics simulations found that strong water/cosolvent attraction leads to co-non-solvency, resulting in both competitive hydrogen bonding and water/cosolvent complexation.[19]

In the presence of a cosolvent, the application of pressure has a dramatic effect on the phase behavior of PNIPAM. Above a certain pressure, the cloud point of a PNIPAM solution is increased (and not decreased, as is the case at atmospheric pressure), and the one phase region is hugely

expanded along the pressure axis.[39,40] Thus, the co-non-solvency effect is reversed at high pressure. Similar to purely aqueous PNIPAM solutions,[41,42,43] the coexistence line in the temperature-pressure frame adopts a convex-upward shape in the presence of a cosolvent.[39,40] The position of the maximum is, however, shifted to significantly higher pressures as well as to higher temperatures, even for systems containing only small fractions of cosolvent.

Application of pressure to aqueous solutions is expected to enhance hydrophobic hydration.[44,45] First, the higher structural order in bulk water weakens the hydrophobic effect,[46,47] and second, the high compressibility of hydration water leads to a tighter packing of water around hydrophobic groups.[48,49,50,51] As a result, the polymer chains stay hydrated in the two-phase region,[52,53] even though the chains collapse,[54] and they form mesoglobules that contain more water than at atmospheric pressure.[53,55] Our recent QENS experiments on a purely aqueous 25 wt% PNIPAM solution[56] showed that the amount of hydration water decreases gradually over a wide temperature range (~20 K) at 130 MPa, in contrast to the abrupt decrease at atmospheric pressure. In the one-phase region, the residence time of the water molecules on the chain is shorter at 130 MPa than at atmospheric pressure, implying weaker constraints at high pressure. Presumably, at high pressure, the polar groups of PNIPAM are less hydrated, while the hydrophobic groups are more hydrated than at atmospheric pressure, consistent with results from other spectroscopic techniques, such as FT-IR spectroscopy[52] and Raman spectroscopy.[53] Recent molecular dynamics simulations align with these findings, suggesting that high pressure increases the water affinity of PNIPAM.[54]

Mechanisms that reduce the total volume of the system may favor the reversal of the co-non-solvency effect at high pressure, because these facilitate a more efficient packing of the small water molecules on the chain.[57,58] Since the volume of a monomer solvated with a cosolvent is relatively large, it is released. This leads to an enrichment of the solvent phase with cosolvent, thereby

reducing the hydrophobic effect and stabilizing the one-phase region.[40,57] This scenario is supported by a Fourier-transform infrared (FT-IR) spectroscopy study of PNIPAM in mixtures of water and methanol,[59] which showed that the fraction of methanol molecules attached to the carbonyl groups of PNIPAM decreases with increasing pressure, while these groups become more hydrated. Partial replacement of cosolvent molecules decorating the PNIPAM chain by water molecules, as pressure is increased, was predicted to reduce bridge formation by cosolvent molecules between distant segments in the PNIPAM chain.[57] In an extension of the adsorption-attraction model, it was suggested that, at high pressure, the interaction strengths between water and the polymer segments as well as those between water and the adsorbed cosolvent are increased, whereas the preferential adsorption of methanol to the polymer and thus the co-non-solvency effect are reduced.[60]

Thus, the interactions of the two solvents with the polymer and with each other, both on the chain and in the bulk solvent mixture, play a role. In our recent SANS experiments on a PNIPAM solution in a water-methanol mixture (80:20 v/v), we characterized the temperature dependence of the concentration fluctuations below the cloud point at various pressures up to 200 MPa.[61] We found that the entropy contribution to the Flory-Huggins segment-segment interaction parameter between the polymer and the solvent mixture decreases with increasing pressure and thus favors demixing of the polymer from the solvent mixture. We attributed this finding to the interaction of the ordered layer of hydration water around the hydrophobic groups of the polymer with the bulk solvent mixture. In the latter, the structure of water may become more ordered upon application of pressure (even in the presence of 20 vol% methanol), which reduces the entropy cost of hydrophobic hydration. At the same time, the enthalpic interactions between the polymer and the

solvent mixture become weaker upon increasing pressure, possibly due to the replacement of hydrogen-bonded water on the chain by methanol, which is less strongly bound to the chain.

While previous experimental work on the effect of pressure on co-non-solvency addressed changes of the polymer, namely its chain conformation[61] and its interactions with water,[59] QENS offers the possibility to simultaneously characterize the dynamics of both bulk and hydration water and to discern the scattering signal of water by using perdeuterated methanol, $CD_3OD$. We choose a high polymer concentration (25 wt%) to be more sensitive to the polymer bound water. For comparison with previous investigations, we investigate a solvent mixture of 80:20 v/v $H_2O/CD_3OD$.[30,59,61] QENS temperature scans with wide ranges of energy transfer across the cloud points at 0.1 and 200 MPa allow a detailed characterization of the dynamics of bulk and hydration water. The analysis is facilitated by converting the dynamic structure factors into susceptibility spectra. Moreover, several water/methanol mixtures are measured, serving as a reference for the dynamics of the water in the bulk solvent mixture in the PNIPAM solution. In addition, Raman spectroscopy in wide temperature ranges across the cloud points at low and high pressure are used to probe the hydration of the hydrophobic groups of PNIPAM. Comparing these results to those from a 25 wt% PNIPAM solution in neat $D_2O$, the influence of methanol on the hydrophobic hydration becomes apparent.

This manuscript is organized as follows. After an Experimental Section, the temperature- and pressure dependent phase behavior of the PNIPAM solution is presented. We discuss the QENS results of the water dynamics in several $H_2O/CD_3OD$ mixtures and the dynamics of $H_2O$ in the PNIPAM solution in 80:20 v/v $H_2O/CD_3OD$. The susceptibility spectra yield relative fractions and relaxation times of the various water species. These are discussed with respect to the changes of hydration and bulk water with temperature and pressure. The insights into the temperature-

dependent hydrophobic hydration from Raman spectroscopy at atmospheric and high pressure are then discussed in comparison with the findings from QENS. Finally, the results are summarized in the Conclusion section.

## Experimental Section

*Materials.* Poly(*N*-isopropylacrylamide) with a molar mass $M_n$ = 36 kg mol$^{-1}$ and a dispersity of 1.26 (end groups carboxylic acid and a hydrogen atom, respectively) was purchased from Sigma-Aldrich. For the solvents, fully deuterated methanol (99.8 % $CD_3OD$, Deutero GmbH), heavy water (99.95 % $D_2O$, Deutero GmbH) or deionized $H_2O$ were used.

For QENS measurements, the polymer was dissolved in 80:20 v/v $H_2O/CD_3OD$ at a concentration of 25 wt% and was shaken for several days prior to the measurements. Neat 80:20 v/v and 70:30 v/v $H_2O/CD_3OD$ solvent mixtures were prepared by mixing at room temperature. For Raman spectroscopy measurements, PNIPAM was dissolved in neat $D_2O$ and in 80:20 v/v $D_2O/CD_3OD$. The use of fully deuterated solvents prevents overlap of the stretching modes of the solvents and the CH stretching modes of PNIPAM.

*Quasi-elastic Neutron Scattering (QENS).* QENS measurements were conducted at the time-of-flight spectrometer TOFTOF at the FRM II, Garching, Germany,[62,63] in the same way as described previously.[56] For the incident neutron beam, a wavelength of 6.0 Å was selected, while the rotation speed of the chopper system was 14,000 rpm. With this configuration, an elastic energy resolution of approximately 0.03 meV (half-width at half-maximum) and energy transfers from -10 to 1.5 meV were obtained. The samples, were mounted in a custom-made aluminum (EN AW-7075) pressure cell, suitable for pressures up to 200 MPa.[64] It was placed at an angle of 135° with respect to the incident neutron beam. Measurements were performed during heating between ~13 and

~57 °C at 0.1 and 200 MPa. (For the determination of the cloud points of the PNIPAM solution at these pressures see Figure S1 in the Supporting Information, SI). The measuring time at each temperature was 120 min with 30 min equilibration time after each temperature change. The signal was recorded with approx. 1000 $He^3$ detector tubes, covering an angle from 7.5 to 140°. The shadow area of the cell around 135° was excluded, which resulted in accessible momentum transfers, $q$, ranging from 0.15 to 1.65 $Å^{-1}$. The time-of-flight spectra were normalized to the incoming neutron flux and a vanadium standard measurement. An empty pressure cell measurement was performed and was subtracted from the data. The time-of-flight data recorded by the detectors were then converted to energy transfers of the neutrons, normalized to the energy-dependent detector efficiency and binned in groups of equal $\Delta q$, resulting in the dynamic structure factor $S(q, \Delta E)$, where $\Delta E$ is the energy transfer. The empty pressure cell and a thin vanadium slab were measured to perform background corrections and calibrations. These operations were carried out using the TOFTOF data reduction routines within Mantid.[65]

From the calculated values of the coherent and incoherent scattering cross sections of the PNIPAM repeating unit, $H_2O$ and $CD_3OD$, it was estimated that 72 % of the detected neutrons were scattered by $H_2O$ (see Tables S1-S3 in the SI). The coherent contributions from all components to the spectra is negligible. For all samples, H-D exchange can be neglected.[30,66]As in our previous work[56] and following well-established protocols,[67,68,69,70] the dynamic structure factors were transformed into the imaginary part of the dynamic susceptibility, $\chi''(q,\nu)$. The frequency $\nu$ is calculated from the energy transfer as $\nu = \Delta E/h$ where $h$ is Planck's constant. $\chi''(q,\nu)$ is related to $S(q,\nu)$ via the relation

$$\chi''(q,\nu) \propto \frac{S(q,-\nu)}{n_B(\nu)} \quad (1)$$

where $n_B$ is the Bose factor,

$$n_B(\nu) = \left[\exp\left(\frac{h\nu}{k_B T}\right) - 1\right]^{-1} \quad (2)$$

with $k_B$ Boltzmann's constant and $T$ the absolute temperature. In this representation, the weighting with the Bose factor reduces the elastic contribution,[71] making the dynamic processes of water more easily discernible. Accordingly, the data are presented and analyzed in the form of susceptibility spectra.

*Raman Spectroscopy.* Raman spectroscopy measurements were performed using the same setup as described previously.[53] A LabRam HR 800 system (JY Horiba) was used in combination with a frequency-doubled Nd:YAG laser with a wavelength of 532 nm, resulting in a spectral resolution of 2 $cm^{-1}$. The laser beam was focused on the sample with a spot size of ~1.5 μm with a power of less than 3 mW. The sample was mounted in a fused silica micro capillary with a squared cross section with inner and outer side lengths of 75 and 350 μm, respectively, which was connected to a pressure generator from High Pressure Equipment Company (Erie, Pennsylvania, U.S.A.). The sample was probed ~20 cm from the interface with the pressurizing medium ethanol. For thermalization, the micro capillary was placed between two copper blocks. The temperature was controlled using a circulating bath thermostat and was measured close to the micro capillary by a Pt 100 resistance thermometer with a precision of 0.2 °C. A possible small temperature offset was corrected employing in-situ micro-turbidimetry. The temperatures at which large aggregates were observed by microscopy were correlated with the cloud points from turbidimetry. Raman spectra were acquired during heating scans between ~19 and ~53 °C at 0.1 and 200 MPa for the 25 wt% solution in 80:20 v/v $D_2O/CD_3OD$ and at 0.1 and 130 MPa for the 25 wt% solution in neat $D_2O$. The integration time was 5 min, following an equilibration time of 10 min after each change of temperature or pressure. A dark count measurement was subtracted from the data. Calibration was performed with a naphthalene standard and the emission lines of a Neon lamp. All spectra were

measured at the same position of the spectrometer without moving the grating between different runs.

## Results and Discussion

### Phase Behavior

We briefly review the temperature-pressure phase diagram of PNIPAM in water/methanol solvents, setting the stage for molecular studies of water dynamics and hydration by QENS and Raman spectroscopy. In a semidilute (3 wt%) solution of PNIPAM in $D_2O/CD_3OD$, $T_{cp}$ increases with pressure from 27.4 °C at atmospheric pressure,[61] reaches a maximum at 231 MPa and 40.2 °C, then decreases to 33.8 °C at 400 MPa (Figure 1). Compared to the coexistence line of a 3 wt% PNIPAM solution in neat $D_2O$,[43] also shown in Figure 1, the one-phase region is largely expanded, while the maximum is shifted to a higher pressure and temperature. At pressures from 0.1 MPa to ~90 MPa, however, the cloud point of PNIPAM in water/methanol is lower than the one in neat water, displaying the co-non-solvency effect. This is reversed at pressures above ~90 MPa, where, in the presence of methanol, the one-phase region is stabilized. The solutions in the present work have a higher polymer concentration, namely 25 wt%. For QENS measurements, they were dissolved in $H_2O/CD_3OD$ instead of $D_2O/CD_3OD$. Nevertheless, the cloud points of the 25 wt% PNIPAM solution in 80:20 v/v $H_2O/CD_3OD$ ($T_{cp}$ = 23.5 ± 0.1 °C and $T_{cp}$ = 40.0 ± 0.1 °C at 0.1 and 200 MPa, respectively) are very close to the coexistence line of the 3 wt% PNIPAM solution in 80:20 v/v $D_2O/CD_3OD$. Also, the cloud points of 25 wt% PNIPAM in $D_2O$ at 0.1 and 130 MPa,[56] resemble the ones of 3 wt% PNIPAM in $D_2O$ (Figure 1).

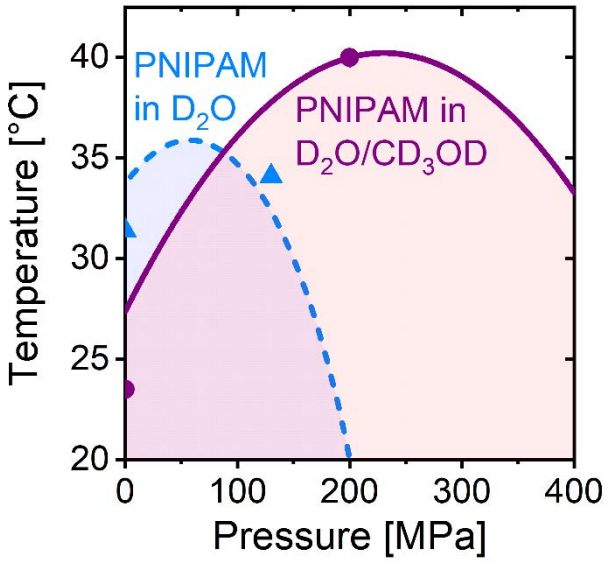


**Figure 1.** Coexistence lines of 3 wt% PNIPAM solutions in 80:20 v/v $D_2O/CD_3OD$ (wine full line, data from ref. 61) and in neat $D_2O$ (blue dashed line, data from ref. 43), as determined using turbidimetry. The shaded and the white areas indicate the one-phase and two-phase regions, respectively. Symbols: cloud points of the 25 wt% PNIPAM solution in $D_2O$ (blue triangles) and in 80:20 v/v $H_2O/CD_3OD$ (wine circles) from turbidimetry. The error bars are smaller than the symbol size.

**Water Dynamics in Water/Methanol Mixtures**

To start with, the dynamics of bulk water in $H_2O/CD_3OD$ mixtures without the polymer were measured by QENS at water/methanol ratios of 80:20 and 70:30 v/v. Figure 2a and b display the dynamic structure factors $S(q,\Delta E)$ of the 80:20 v/v $H_2O/CD_3OD$ mixture at a $q$ value of 1.55 $Å^{-1}$ at 0.1 MPa and 200 MPa in dependence on temperature. At both pressures, slight changes are observed with increasing temperature: The intensity decreases at very low energy transfers (below ~0.2 meV), while it increases at higher values.

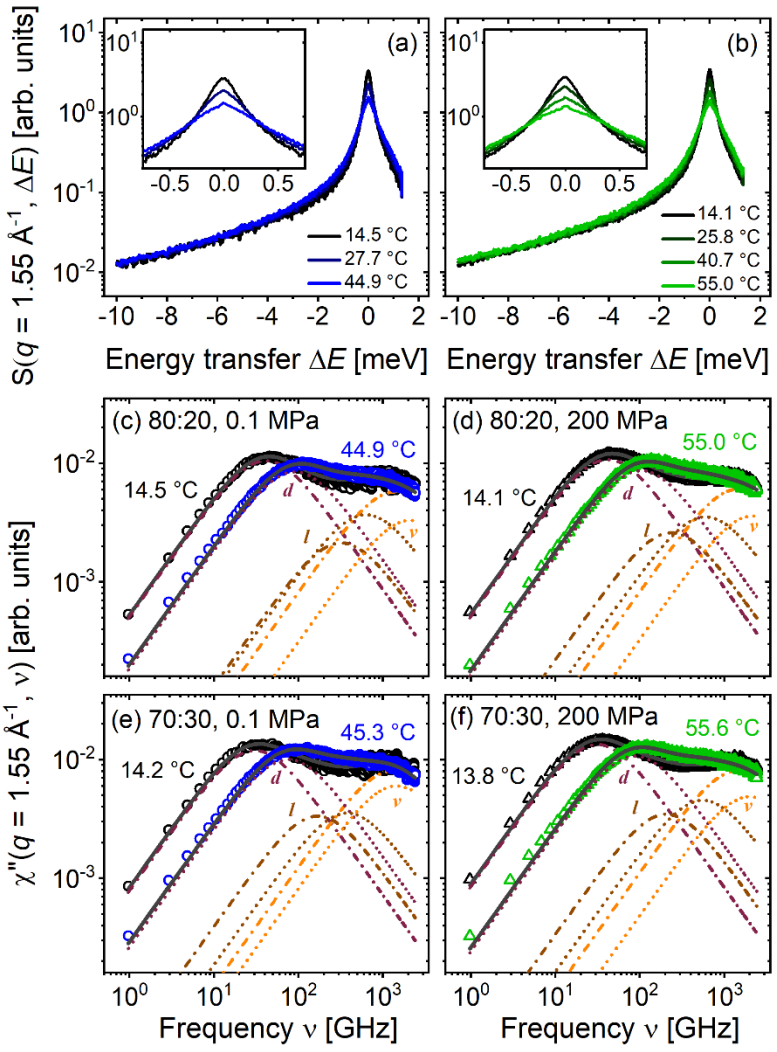


**Figure 2.** (a,b) Dynamic structure factors, $S(q,\Delta E)$, of the 80:20 v/v $H_2O/CD_3OD$ obtained at $q$ = 1.55 Å$^{-1}$ at 0.1 MPa (a) and 200 MPa (b) at the temperatures indicated in the graphs. The insets show $S(q,\Delta E)$ at small energy transfers. (c-f) Imaginary part of the dynamic susceptibility, $\chi''(q,\nu)$ of the 80:20 (c, d) and the 70:30 v/v $H_2O/CD_3OD$ mixtures (e, f), determined according to eqs 1 and 2, at 0.1 MPa (c, e) and 200 MPa (d, f), both at $q$ = 1.55 Å$^{-1}$ and at the temperatures given in the graphs. The lines are the overall fits of eq 3 (full grey lines) and their individual contributions: diffusional process *d* (wine lines), local process *l* (brown lines) and the vibrational process *v* (orange lines) at low temperature (dashed-dotted lines) and high temperature (dotted lines).

The dynamic structure factors $S(q,\Delta E)$, obtained from the QENS measurements, were transformed into the imaginary part of the corresponding dynamic susceptibility, $\chi''(q,\nu)$. The susceptibility spectra of the two $H_2O/CD_3OD$ mixtures at selected temperatures at 0.1 MPa (Figure 2c and e) and 200 MPa (Figure 2d and f) at $q$ = 1.55 Å$^{-1}$ feature two distinct peaks, as for neat water.[56] The susceptibility spectra for other $q$ values are shown in Figures S2 and S3 in the SI. The peak at low frequencies is related to the diffusion of water molecules. With increasing temperature, this contribution shifts to higher frequencies at both pressures, indicating a faster diffusion. The peak at high frequencies is due to vibrational processes, and their positions do not show a pronounced temperature dependence.

As in neat $H_2O$,[56,69] the deconvolution of the data reveals three water relaxation processes in the frequency range from 1 to ~5000 GHz: a diffusional process ($d$) centered at ~$8\times10^1$ GHz, an effective local process ($l$) centered at ~$3\times10^2$ GHz, and a vibrational process ($v$) centered at ~$2\times10^3$ GHz. Therefore, the susceptibility spectra are modelled as

$$\chi''_q(\nu)=\chi''_{q,d}(\nu) + \chi''_{q,l}(\nu) + \chi''_{q,v}(\nu). \quad (3)$$

As in our previous work,[56] the diffusional and the effective local processes are parametrized by Debye functions (eq S1 in the SI),[72] which describe a homogeneous relaxation process, i.e., a single exponential in the time domain. It includes the relaxation time, $\tau_i$, and a scaling constant, $C_{q,i}$, where the index $i$ stand for $d$ or $l$. We note that the diffusion of methanol may give a weak contribution having a peak frequency similar to the one of the diffusional process of water;[73] however, from the scattering cross sections (Tables S1-S3 in the SI), its contribution is expected to be too weak to significantly alter the results. The vibrational process of water, described by a damped harmonic oscillator (DHO) function (eq S2 in the SI),[74] accounts for intermolecular O-O-O bending vibrations in the hydrogen bonding network.[75,76,77] (see the broken lines in Figure 2c-

f). The resulting relaxation times of the diffusion process of the water molecules, $\tau_d$, are shown for both pressures in Figure 3 as a function of temperature. The $q$ dependence of $\tau_d$, shown in Figure S4 in the SI, reveals, that at low $q$ values, the slope of $\tau_d$ approaches $q^{-2}$ in all cases, indicating long-range diffusion of the water molecules.[78] (The temperature-dependent relaxation times of the local process, $\tau_l$, are shown in Figure S5 in the SI.) The behavior of $\tau_d$ shows three distinct features. First, with increasing temperature, $\tau_d$ decreases for all samples and both pressures, as expected.[79] Second, with increasing methanol content, $\tau_d$ increases, in consistency with previous QENS measurements on water-alcohol mixtures at atmospheric pressure.[80] Thus, the average relaxation time of the water molecules slows down with increasing methanol content, which is due to an altered local structure around the water molecules. No change in the shape of the relaxation time distribution with methanol content was observed. Previous studies on methanol-poor mixtures suggest that water and methanol form complexes with composition depending on the methanol content and temperature.[81,82] In other studies, it was observed that water forms distorted cages that encapsulate methanol molecules.[83,84] Third, we observed that the application of high pressure (200 MPa) does not alter $\tau_d$ significantly. In neat water, the transition of the hydrogen bond network from an open tetrahedral to a more compact coordination becomes apparent at ca. 200 MPa at room temperature.[47,85] In water/alcohol mixtures, notable changes in interactions occur at pressures of similar magnitude, as inferred from Raman measurements.[86,87] Thus, even though structural changes in the solvent mixture may occur at 200 MPa, the relaxation of water is affected only marginally. Within these limitations, we use the value of $\tau_d$ to estimate the water/methanol ratio of the bulk solvent phase in the PNIPAM solution shown below.

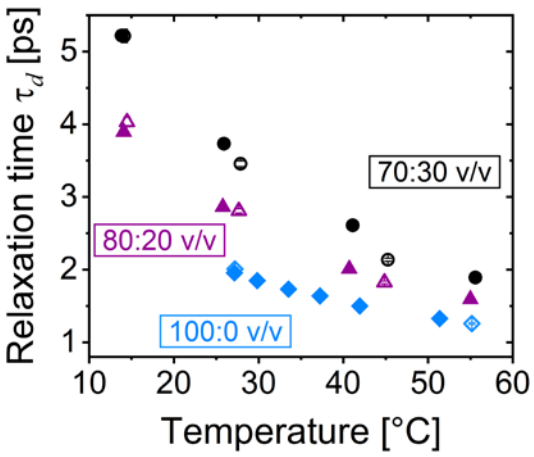


**Figure 3.** Relaxation time of the diffusive mode of $H_2O$ molecules, $\tau_d$, at $q$ = 1.55 Å$^{-1}$ in 70:30 v/v $H_2O/CD_3OD$ (black circles), 80:20 v/v $H_2O/CD_3OD$ (purple triangles) and in neat $H_2O$ (light blue diamonds) as a function of temperature at 0.1 MPa (open symbols), at 200 MPa for 70:30 v/v and 80:20 v/v, and at 130 MPa for neat $H_2O$ (closed symbols). The data from neat $H_2O$ are taken from Ref. 56.

At atmospheric pressure, the formation of clusters from water and methanol molecules was proposed to be the driving force for the co-non-solvency effect.[37,38] These clusters should form a new species that acts as a poor solvent for the chains. It was suggested that these clusters disintegrate at high pressure, allowing individual methanol molecules to interact with the chains, which leads to an increased cloud point.[16] This is, however, at variance with the observation that $\tau_d$ does not significantly change with pressure between 0.1 and 200 MPa. Therefore, the pressure dependence of the co-non-solvency effect cannot be predominantly attributed to solvent-solvent interactions and clusters.

**Dynamic Susceptibility Spectra of PNIPAM in Water/Methanol Mixtures**

We now turn to the dynamics of water in the PNIPAM solution in mixed solvents. Figures 4a and b display the dynamic structure factor $S(q,\Delta E)$ of the 25 wt% PNIPAM solution in 80:20 v/v $H_2O/CD_3OD$ at $q$ = 1.55 Å$^{-1}$ at 0.1 MPa and 200 MPa in dependence on temperature. In comparison with $S(q,\Delta E)$ of the neat 80:20 v/v $H_2O/CD_3OD$ mixture, an enhanced intensity is observed at very low energy transfers (between -0.25 and 0.25 meV), which points to the presence of very slowly moving moieties. At both pressures, slight changes are discernible with temperature. Above $T_{cp}$, the intensity at very low energy transfers (below ~0.2 meV) decreases, whereas the one at higher energy transfers increases.

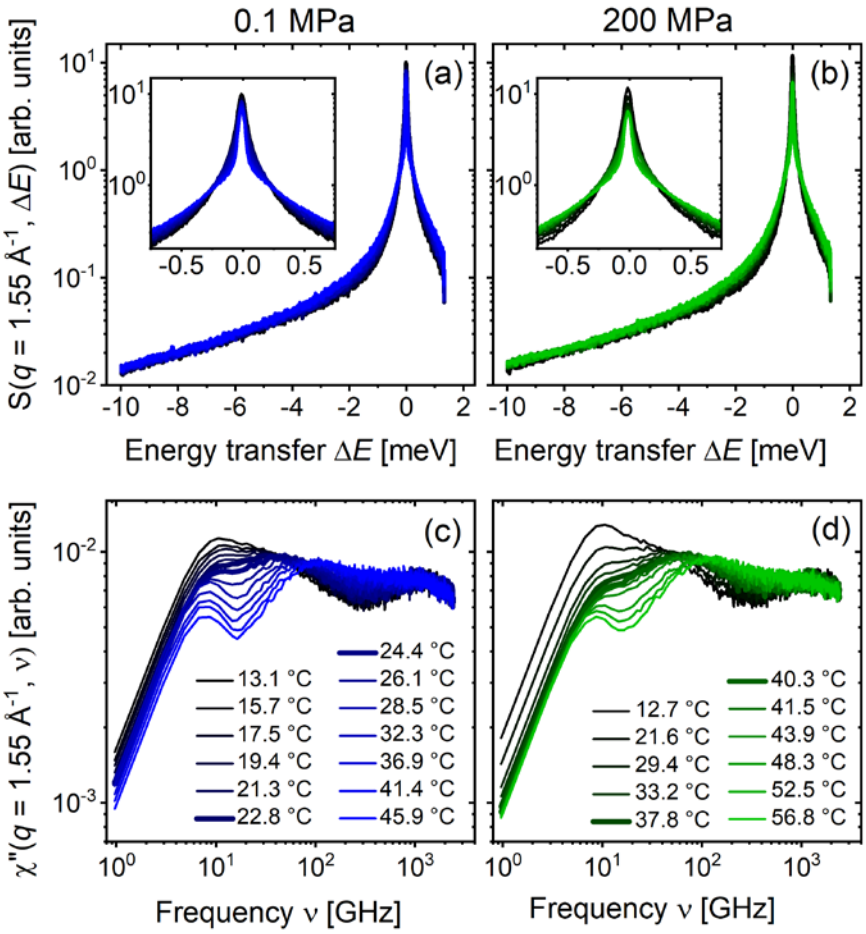

**Figure 4.** Dynamic structure factors $S(q,\Delta E)$, (a,b), and the imaginary part of the dynamic susceptibility $\chi''(q,\nu)$, (c,d), of the 25 wt% PNIPAM solution in 80:20 v/v $H_2O/CD_3OD$ obtained at $q$ = 1.55 Å$^{-1}$ at 0.1 MPa (a,c) and 200 MPa (b,d) at the temperatures indicated in panel (c) and (d). The curves just below and just above the respective cloud point are highlighted in bold. The insets in (a) and (b) show $S(q,\Delta E)$ at small energy transfers.

The dynamic structure factors are converted into susceptibility spectra, $\chi''(q,\nu)$, according to eqs 1 and 2, as before. These are shown in Figure 4 for the measurements at 0.1 MPa (Figure 4c) and at 200 MPa (Figure 4d). At low temperatures, i.e., in the one-phase region, strong contributions at low (~10 GHz) and high frequencies (~1000 GHz) are present at both pressures. The contribution at low frequencies is due to the relaxation of hydration water,[56,88] i.e., water molecules that are associated to the polymer chains. The high-frequency contributions are due to dynamic processes in the bulk solvent. Their intensity is lower than in the spectra of the neat 80:20 $H_2O/CD_3OD$ solvent mixture (Figure 2c and d), implying that only a rather small amount of bulk water molecules is present in the one-phase region at both pressures. Over the entire temperature range and at both pressures, the intensity at low frequencies decreases, whereas the one at higher frequencies increases. Thus, upon heating, water is released from the chains and adds to the bulk solvent phase. At atmospheric pressure and at temperatures above $T_{cp}$ (23.5 ± 0.1 °C), there is a pronounced intensity decrease at low frequencies, pointing to a strong dehydration of the chains. In contrast, at high pressure, this intensity decrease is gradual over the entire temperature range, including the cloud point at $T_{cp}$ = 40.0 ± 0.1 °C. At both pressures, a contribution at frequencies below 10 GHz remains over the whole temperature range. This reveals the presence of very slowly moving moieties with dynamics that cannot be resolved with the time-of-flight spectrometer.

Over the entire frequency range (1 to ~5000 GHz) of the susceptibility spectra, five relaxation processes can be distinguished and deconvoluted: An elastic contribution (*el*) at frequencies within the resolution limit, a relaxation process of hydration water (*h*) centered at ~$10^1$ GHz, a diffusional process of bulk water (*d*) centered at ~$8\times10^1$ GHz, an effective local process of bulk water (*l*) centered at ~$3\times10^2$ GHz, and a vibrational process (*v*) centered at ~$2\times10^3$ GHz. Therefore, the susceptibility spectra of the PNIPAM solution were modelled with the expression:

$$\chi''_q(\nu) = \chi''_{q,el}(\nu) + \chi''_{q,h}(\nu) + \chi''_{q,d}(\nu) + \chi''_{q,l}(\nu) + \chi''_{q,v}(\nu) \quad (4)$$

The elastic contribution is indistinguishable from the resolution function, measured with a vanadium standard. Therefore, it is represented by the measured resolution function in the deconvolution of the dynamic susceptibility, and its amplitude $C_{q,el}$ is varied in the fits:[89]

$$\chi''_{q,el}(\nu) = C_{q,el} \cdot \chi''_{q,Res}(\nu) \quad (5)$$

To account for dynamic heterogeneity, the relaxation of hydration water is parametrized by a Cole-Davidson function (eq S3 in the SI), which includes the relaxation time of hydration water, $\tau_h$, and a scaling constant, $C_{q,h}$.[72] As for the purely aqueous PNIPAM solution,[56] the Cole-Davidson stretching exponent, α, was kept fixed at 0.7 for all spectra (for details see ref 56). Both the diffusional process and the effective local process of bulk water are parametrized by Debye functions (eq S1 in the SI), and the vibrational relaxation process by a DHO function (eq S2 in the SI). As water and methanol are bound to the polymer chains or are released, the solvent composition changes, which may have an influence on the dynamics of $H_2O$ in the bulk solvent mixture. This was taken into account when fitting these contributions; only the value of $\tau_l$ was kept fixed at the values obtained for the 80:20 v/v $H_2O/CD_3OD$ solvent mixture without the polymer, because of the low absolute intensity of the effective local process. This allows a reliable determination of the other fitting parameters. Treating the relaxation time of the diffusive mode of

$H_2O$ molecules in the bulk solvent phase, $\tau_d$, as a fitting parameter is found to cause instabilities in the fits of the spectra at low momentum transfers. Therefore, only the spectra at $q$ = 1.45, 1.55 and 1.65 $Å^{-1}$ are analyzed. The presented results are averaged values resulting from the measurements at these $q$ values.

Representative fits of eq 4 to the data are shown for the measurements at 0.1 MPa (Figure 5a-c) and at 200 MPa (Figure 5d-f), both in the one-phase and two-phase regions. Irrespective of pressure, the spectra in the one-phase region (panels a, d, e) are dominated by the contribution from hydration water. In the two-phase region, it is strongly decreased at both pressures, but remains present, and the intensities of the diffusional and the effective local process of bulk water are increased. Thus, at $T_{cp}$, a fraction of the hydration water in the one-phase region is released from the chains and joins the bulk solvent phase. At none of the pressures, the intensity of the vibrational process is significantly affected by the increase in temperature. We note that possible contributions from the polymer dynamics cannot be completely excluded. However, these are expected at frequencies lower than the range probed here.[88,90]

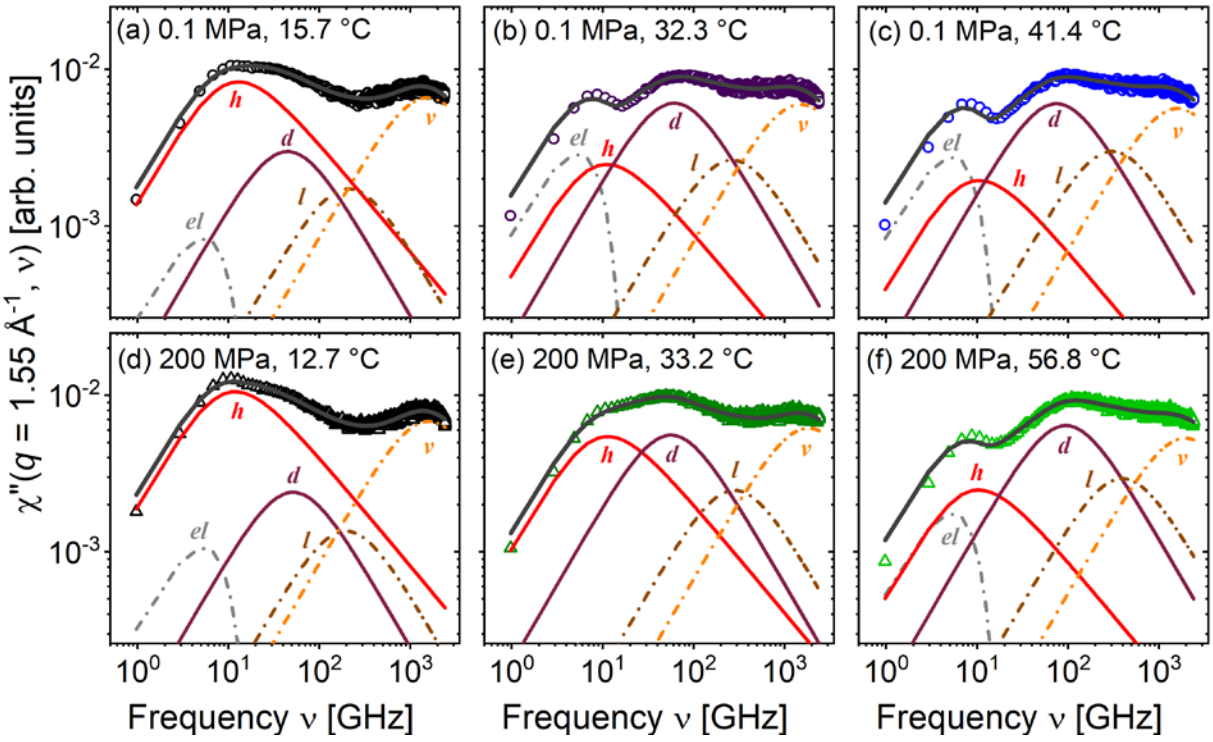


**Figure 5.** Example fits of $\chi''(q,\nu)$ of the 25 wt% PNIPAM solution in 80:20 v/v $H_2O/CD_3OD$ in the one-phase region at 0.1 MPa at 15.7 °C (a) and at 200 MPa at 12.7 °C (d) and 33.2 °C (e), and in the two-phase region at 0.1 MPa at 32.3 °C (b) and 41.4 °C (c) and at 200 MPa at 56.8 °C (f). Data (open symbols), fits of eq 4 (dark grey lines) and their individual contributions: Elastic fraction *el* (grey), relaxation process of hydration water *h* (red), diffusion process of bulk water *d* (wine), local process of bulk water *l* (brown) and the vibration process *v* (orange). In (e), the elastic contribution is very weak.

**Temperature and Pressure Dependence of the Elastic Scattering**

The elastic line strength $C_{q,el}$ (eq 5) is shown as a function of temperature in Figure 6a and b. In the one-phase region it decreases slightly with increasing temperature at both pressures. Above $T_{cp}$, it increases sharply at 0.1 MPa, until a plateau is reached at ~30 °C. In contrast, $C_{q,el}$ increases gradually at 200 MPa. This difference reflects the characteristic influence of pressure on the phase

transition, which is sharp at 0.1 MPa, but spans over a broad temperature range at 200 MPa, similarly to purely aqueous PNIPAM solutions.[56]

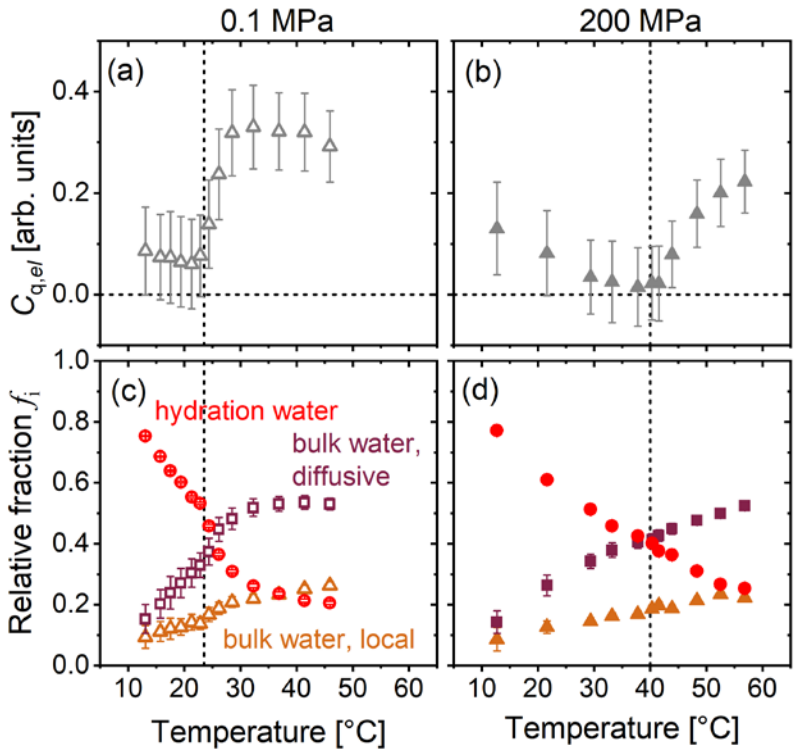


**Figure 6.** Upper panels: Elastic line strength $C_{q,el}$ in the 25 wt% PNIPAM solution in 80:20 v/v $H_2O/CD_3OD$ at 0.1 MPa (a) and 200 MPa (b) as a function of temperature. Lower panels: Relative populations $f_i$ of different water species as a function of temperature at 0.1 MPa (c) and 200 MPa (d). Red circles: Hydration water (*h*); wine squares: diffusive contribution to bulk water (*d*); and brown triangles: effective local contribution to bulk water (*l*). The cloud points are indicated by the vertical dashed lines.

The increase of $C_{q,el}$ at $T_{cp}$ may be attributed to a reduced mean-square displacement of hydrogen atoms. This is expected in the two-phase region due to chain collapse. It enhances the Debye-Waller prefactor and, therefore, the elastic line strength. In addition, water molecules may be

trapped inside the polymer-rich domains above $T_{cp}$, which strongly hinders their motion. It is also conceivable that dynamic modes of the polymer that were faster than the resolution limit in the one-phase region may be hindered in the two-phase region, thereby contributing to the elastic scattering. For instance, the side groups of PNIPAM may be involved in a relatively fast dynamic process below $T_{cp}$, but their motion may be restricted above. However, due to the low frequencies of dynamic processes of the chains already in the one-phase region,[29] this contribution presumably plays only a minor role.

**Relative Populations of Bulk and Hydration water**

In this section, we analyze the temperature dependence of the relative fractions of different water species $f_i$ across the cloud points at 0.1 and 200 MPa. These are determined from the amplitudes of the individual contributions to the susceptibility spectra $C_i$, where the index *i* stands for *h*, *d* or *l*. Since the amplitudes $C_i$ are proportional to the scattering intensities of the respective water species, the relative populations of the different types of hydration and bulk water, $f_i$, are determined as[56]

$$f_i = \frac{C_{q,i}}{C_{q,h}+C_{q,d}+C_{q,l}} \quad (6)$$

using again the averaged values at $q$ = 1.45, 1.55 and 1.65 Å$^{-1}$. Here, the vibrational process is not included, as it may contain contributions from both hydration water and bulk water. The total number of water molecules considered for the determination of $f_i$ can be assumed constant. While very strongly bound water may be included in the elastic line, this amount is presumably negligible in comparison with $f_d$ and $f_h$. Changes of the fraction of bound water ($f_h$) result in opposite changes in the fraction of the contributions from bulk water, $f_d$ and $f_l$.

The resulting relative fractions $f_h$, $f_d$ and $f_l$ are shown as a function of temperature at both 0.1 and 200 MPa in Figure 6c and d. In the one-phase region at 0.1 MPa, $f_h$ decreases with temperature from a value of ~0.8 at 13.1 °C to ~0.5 at $T_{cp}$, reflecting the decreased intensity of the susceptibility at low frequencies (Figure 4c and d). At a pressure of 200 MPa, the fraction of hydration water mimics its behavior at 0.1 MPa at the lowest measured temperatures, however, it decreases more gradually, as $T_{cp}$ is approached.

The change of $f_h$ near the respective cloud point temperatures $T_{cp}$ is very different for the two pressures: At 0.1 MPa, $f_h$ decreases abruptly at $T_{cp}$, then flattens off within 5 K above $T_{cp}$ and reaches a constant value of ~0.2 at 45.9 °C. At 200 MPa, the decrease of $f_h$ is much less abrupt above $T_{cp}$, though it continues to decrease steadily in the two-phase region, even up to 15 K above $T_{cp}$. At both pressures, $f_h$ converges towards a finite value. This is consistent with the kinetically trapped water,[53] or water that remains hydrogen bonded with hydrophilic groups,[20] observed in purely aqueous PNIPAM solutions at atmospheric pressure. Moreover, the relatively sharp transition at 0.1 MPa in comparison with 200 MPa reflects the narrower temperature range in which phase separation takes place, as observed in purely aqueous PNIPAM solutions.[56] The bulk water fractions $f_d$ and $f_l$ show similar behavior: At both pressures, they increase in the entire temperature range. At the cloud point at 0.1 MPa, they increase sharply, whereas at 200 MPa, the increase is gradual.

These results can be connected with our previous small-angle neutron scattering study on the pressure dependence of the co-non-solvency effect of PNIPAM in a water/methanol mixture.[61] It was found that, at high pressure, the correlation length of concentration fluctuations in the one-phase region is larger than at low pressure. Thus, at high pressure, chains in the one-phase region are not solvated as strongly as at low pressure. This is consistent with the reduced value of $f_h$ in

the one-phase region at 200 MPa, which becomes apparent when plotting $f_h$ as a function of the temperature interval to $T_{cp}$ (see Figure S6 in the SI).

**Bulk Water Dynamics in PNIPAM/Water/Methanol Mixtures**

The binding or release of water and methanol to the PNIPAM chains alters the composition of the bulk solvent, which is expected to be reflected in the relaxation time $\tau_d$ of the water molecules in the bulk solvent phase. Using the measured data from the neat 80:20 and 70:30 v/v $H_2O/CD_3OD$ solvent mixtures as a reference we can estimate the effective bulk solvent composition in the PNIPAM solution in dependence on temperature and pressure. Figure 7a and b depict $\tau_d$ in the polymer solution as a function of temperature at 0.1 MPa and 200 MPa along with the relaxation times measured in the neat 80:20 and 70:30 v/v $H_2O/CD_3OD$ solvent mixtures. In the neat solvent mixtures, the average relaxation time $\tau_d$ increases with methanol content, i.e., water molecules diffuse more slowly in the presence of methanol.

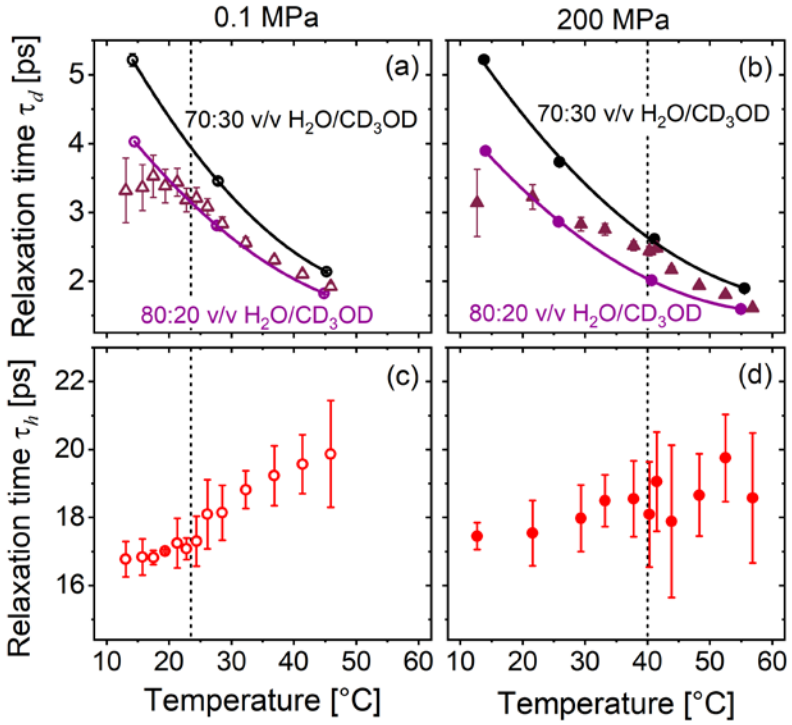

**Figure 7.** (a,b) Relaxation time of the diffusive mode of $H_2O$ molecules in the bulk solvent phase, $\tau_d$, of the 25 wt% PNIPAM solution in 80:20 v/v $H_2O/CD_3OD$ (wine triangles), of the 80:20 (purple circles) and of the 70:30 v/v $H_2O/CD_3OD$ mixture (black circles), as a function of temperature at 0.1 MPa (a) and 200 MPa (b). The purple and black lines are guides to the eye. (c,d) Relaxation time of hydration water, $\tau_h$, in the 25 wt% PNIPAM solution in 80:20 v/v $H_2O/CD_3OD$ at 0.1 MPa (c) and 200 MPa (d) as a function of temperature. The dashed vertical lines mark the cloud points of the polymer solution at both pressures.

At 0.1 MPa (Figure 7a), the values of $\tau_d$ in the PNIPAM solution are lower than the ones of the neat 80:20 v/v $H_2O/CD_3OD$ solvent mixture, they reach the same values as in the neat 80:20 v/v $H_2O/CD_3O$ mixture near $T_{cp}$ in the one-phase region at ~20 °C, and become slightly larger above 30 °C, i.e., deep in the two-phase region. Thus, at low temperatures, the methanol concentration in the solvent phase is lower than the stoichiometric one, i.e., a large fraction of methanol is localized at the PNIPAM chains. This finding lends support to the notion that the co-non-solvency effect at atmospheric pressure is mainly due to preferential adsorption of the organic solvent on the chains in the one-phase region.[9,33] Near $T_{cp}$, neither solvent is preferentially adsorbed at the chains: Both in the solvent and at the chains, water and methanol are present with an 80:20 v/v composition. Deep in the two-phase region (above 30 °C), methanol molecules are more strongly expelled from the polymer-rich domains than water molecules, leading to an effectively larger methanol concentration in the bulk solvent phase at high temperatures.

At 200 MPa, different behavior is observed (Figure 7b). At low temperatures, $\tau_d$ of the PNIPAM solution is close to that of neat 80:20 v/v $H_2O/CD_3OD$. At temperatures of 30 °C and above, $\tau_d$ increases above the values of the neat 80:20 v/v $H_2O/CD_3OD$ mixture. At $T_{cp}$, $\tau_d$ reaches nearly the same value as in the neat 70:30 v/v $H_2O/CD_3OD$ mixture. Thus, near $T_{cp}$, the bulk solvent

phase is enriched with methanol, which, in turn, means that water is preferentially adsorbed on the polymer chains. This supports models attributing the reversal of the co-non-solvency effect at high pressure to enhanced polymer-water interactions.[57,58,60] Over a temperature interval of 20 °C above $T_{cp}$, $\tau_d$ gradually approaches the same value as in the neat 80:20 v/v $H_2O/CD_3OD$ mixture, i.e., the original solvent partitioning is regained.

These results allow for an estimate of the effective solvent composition adsorbed on the polymer chains at 200 MPa. By assuming that all methanol molecules are released from the chains near $T_{cp}$, we find from the value of $f_h$ of 0.4 (Figure 6d), that the bulk solvent mixture has a composition of 71:29 v/v water/methanol (see the SI and Figure S7 for a detailed calculation). This ratio is very similar to the one deduced from the measured relaxation time of water in the bulk solvent mixture near $T_{cp}$ at 200 MPa $\tau_d$ (Figure 7b). It can be concluded that nearly all methanol molecules are expelled from the chains near $T_{cp}$ at 200 MPa. This pressure is close to the pressure at which the maximum of the coexistence line in the temperature-pressure frame is located (231 MPa, Figure 1), i.e., at this pressure the co-non-solvency effect is maximally reversed. Therefore, the observed replacement of the majority of methanol by water on the chains at 200 MPa confirms the dominant role of preferential water adsorption for the breakdown of the co-non-solvency effect at high pressure.

**Hydration Water Dynamics in PNIPAM/Water/Methanol Mixtures**

In addition to the relative fraction of the hydration water discussed above, the susceptibility spectra yield information on the relaxation time, $\tau_h$, of hydration water (Figure 7c and d), which provide additional insights into the polymer-solvent interactions. At both pressures, $\tau_h$ increases with temperature over the entire range. However, they show several differences: (i) At 0.1 MPa,

the values of $\tau_h$ below and at $T_{cp}$ are significantly lower than at 200 MPa. For instance, at $T_{cp}$, $\tau_h$ = 17.1 ± 0.4 ps at 0.1 MPa, but 18.5 ± 0.8 ps at 200 MPa. (ii) $\tau_h$ increases abruptly at $T_{cp}$, while it increases steadily at 200 MPa. (iii) Above $T_{cp}$, $\tau_h$ increases at 0.1 MPa, with a lower slope than below, while it levels off at 200 MPa.

We first discuss the behavior at 0.1 MPa. Since the hydrogen bonds of $H_2O$ with the amide groups of PNIPAM restrict the motion of the water molecules more than the hydrophobic groups,[91,92,93] the sudden increase of $\tau_h$ at $T_{cp}$ suggests that the amide groups mainly stay hydrated, whereas the hydrophobic groups are abruptly dehydrated,[56] leading to an overall increased $\tau_h$. Moreover, as recently found in atomistic computer simulations,[36] the dynamics of the water molecules near the chain may be influenced by interactions with nearby alcohol molecules. In addition, in the two-phase region, water molecules may be trapped inside the polymer-rich phase,[56] contributing to the steady increase of the relaxation time above $T_{cp}$.

At 200 MPa, larger $\tau_h$ values are observed below and at $T_{cp}$ than at 0.1 MPa. This becomes especially evident when comparing the values at same temperature interval with respect to $T_{cp}$ (see Figure S6 in the SI). Two effects may be at the origin. First, as discussed above, a longer relaxation time may point to an enhanced hydrophilic hydration, implying that the application of pressure favors hydrophilic hydration compared to hydrophobic hydration. As will be discussed below, this is not in line with Raman spectroscopy of the methyl group vibrations. Second, the relaxation dynamics of hydration water at the chains is affected by the presence of methanol. In the one-phase region, more methanol is preferentially adsorbed on the chain at low pressure than at high pressure (Figure 7a and b). Therefore, both species are present on the chains in significant amount at low pressure, which may weaken the interaction strength between water and PNIPAM. This could be due to a significant influence of adsorbed methanol molecules on the interaction strength between

PNIPAM and water, thereby shortening $\tau_h$. Furthermore, the presence of a weakly bound hydration shell around methanol molecules that are adsorbed on the chains may overlap with the signal from polymer bound water, leading to an apparent shortening of $\tau_h$. As shown above, at 200 MPa nearly all methanol molecules are expelled from the chains, diminishing these effects.

**Hydrophobic Hydration in PNIPAM/Water/Methanol Mixtures**

From QENS, it became evident that hydrophilic and hydrophobic hydration of PNIPAM in a water/methanol mixture behave differently at low and high pressure, when the solution is heated through $T_{cp}$. Further insight on the hydrophobic hydration of PNIPAM in an 80:20 v/v water/methanol solvent mixture is gained from Raman spectroscopy by probing the vibrations of the methyl groups of the polymer. For comparison, results from a purely aqueous PNIPAM solution are presented. The Raman spectra of the 25 wt% PNIPAM solution in neat $D_2O$ and in 80:20 v/v $D_2O/CD_3OD$ at different temperatures for pressures of 0.1 and 130 MPa, and 0.1 and 200 MPa, respectively, are shown in Figure 8. To compare with a purely aqueous PNIPAM solution, we chose a pressure of 130 MPa, because it is near the pressure where the coexistence line has its maximum, as for the PNIPAM solution in the solvent mixture (Figure 1).

In the CH stretching region, four bands are discernible. They are assigned to the symmetric stretching mode of $CH_3$ in the side groups ($\nu_s(CH_3)$ at ~2878 $cm^{-1}$), to the CH stretching vibrations in the backbone and in the side groups ($\nu(CH)$ at 2922 $cm^{-1}$), the antisymmetric stretching modes of $CH_2$ in the backbone ($\nu_{as}(CH_2)$ at 2945 $cm^{-1}$) and of $CH_3$ in the side groups ($\nu_{as}(CH_3)$ at 2985 $cm^{-1}$).[20,94,95] As deuterated methanol is used, the vibrational modes of its hydrophobic groups are shifted to lower frequencies due to the isotope effect and do not overlap with the polymer C-H vibrations. The cloud point temperatures were determined in situ by optical microscopy. For 25

wt% PNIPAM in neat $D_2O$, $T_{cp}$ = 32.2 ± 0.6 and 35.1 ± 0.7 °C at 0.1 and 130 MPa, respectively, whereas for 25 wt% PNIPAM in 80:20 v/v $D_2O/CD_3OD$, $T_{cp}$ = 25.2 ± 0.8 and 39.8 ± 0.9 °C at 0.1 and 200 MPa, respectively.

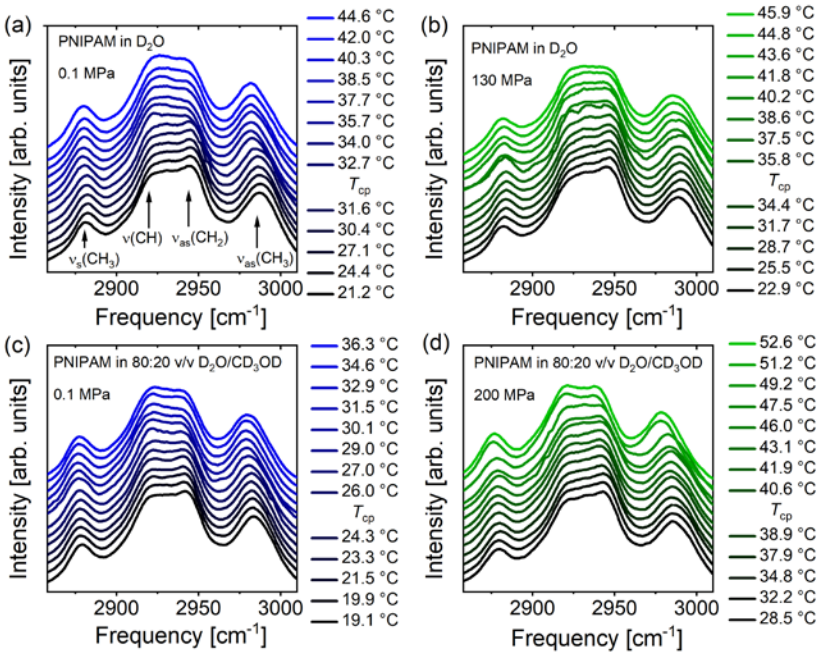


**Figure 8.** Raman spectra of the 25 wt% PNIPAM solution in neat $D_2O$ at 0.1 MPa (a) and 130 MPa (b) and in 80:20 v/v $D_2O/CD_3OD$ at 0.1 MPa (c) and 200 MPa (d), in the CH stretching region in dependence on temperature. The temperature of each curve and the relative position of the respective cloud points, as determined by in-situ optical microscopy, are indicated in the graphs. For clarity, the curves are shifted in intensity and smoothened using the Savitzky-Golay algorithm.

Small changes in the spectral bands are observed with increasing temperature at both low and high pressure in the two samples. At 0.1 MPa, the positions of all four bands are approximately constant in the one-phase region. At the respective cloud points in the two samples, the positions of the $\nu_{as}(CH_3)$ mode shift abruptly to slightly lower wavenumbers, and then remain again constant. At high pressure for the two samples, the frequencies of both vibrational modes decrease as well, but in a gradual manner. The $\nu_s(CH_3)$, $\nu(CH)$ and $\nu_{as}(CH_2)$ modes do not display notable changes

in any case. The strong decrease in the peak frequencies of the two vibrational modes at 200 MPa and $T_{cp}$ + ~10 K for the 25 wt% PNIPAM solution in 80:20 v/v $D_2O/CD_3OD$ might suggest the presence of a second transition (see also Figure 9). Since it was not observed in the QENS experiments, it could be caused by the interaction with the inner surfaces of the glass capillary used for Raman spectroscopy. The inner diameter of the capillary (~100 μm) is of the same order of magnitude as the size of the polymer-rich domains in the two-phase region, which might result in local variations in the composition.

The Raman spectra were deconvoluted by a superposition of four Voigtian lineshapes (eqs S12-S15 and Figures S8 and S9 in the SI). Figure 9 shows the resulting peak frequencies of the $\nu_{as}(CH_2)$ and the $\nu_{as}(CH_3)$ vibrational modes of the backbone and the side groups, respectively, as a function of temperature. The C-H bond lengths in the hydrophobic groups increase when they are hydrated, i.e., hydrogen bonds between these groups and $D_2O$ are improper.[96,97,98,99] Thus, the decreasing frequencies of the $\nu_{as}(CH_2)$ and the $\nu_{as}(CH_3)$ modes point to dehydration of these groups.

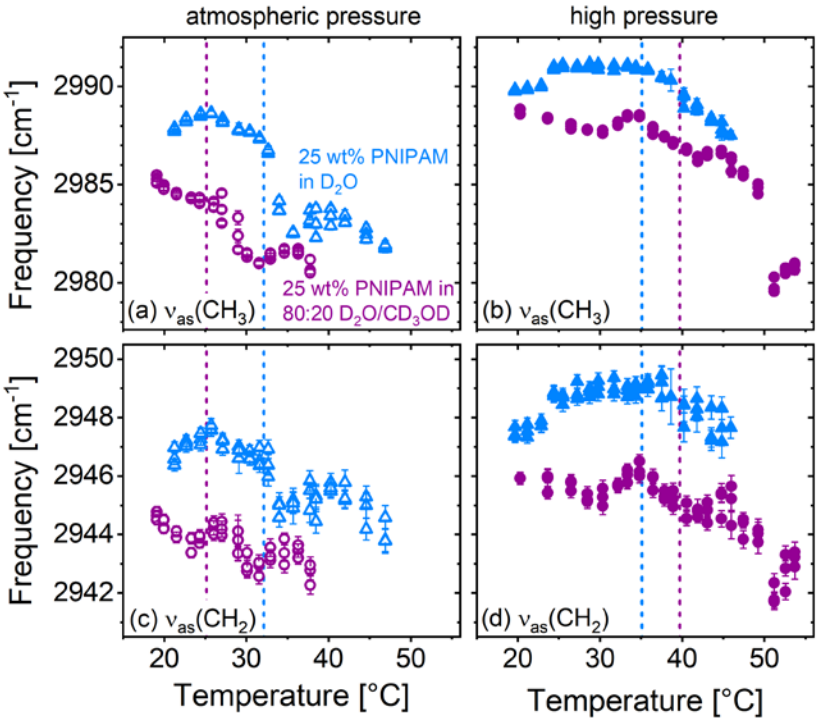

**Figure 9.** Peak frequencies $\nu_{as}(CH_3)$ (a, b) and $\nu_{as}(CH_2)$ (c, d) of the 25 wt% PNIPAM solution in 80:20 v/v $D_2O/CD_3OD$ (purple circles) at 0.1 (a,c) and 200 MPa (b,d), and of the 25 wt% PNIPAM solution in neat $D_2O$ (light blue triangles) at 0.1 MPa (a,c) and 130 MPa (b,d) as a function of temperature. The dashed vertical lines mark the cloud points at both pressures.

We discuss the 25 wt% PNIPAM solution in neat $D_2O$ first. The behavior of the $\nu_{as}(CH_3)$ mode in this solution (Figure 9a and b) is reminiscent of the one in a 3 wt% solution observed by us previously:[53] At atmospheric pressure, its frequency decreases abruptly at $T_{cp}$ and remains constant above. In contrast, at 130 MPa, the decrease in frequency sets in at $T_{cp}$, is gradual and spans over more than 10 K, i.e., the phase transition extends over a broad temperature range. In the one-phase region, however, the frequency is slightly lower than in the 3 wt% PNIPAM solution in $D_2O$,[53] suggesting that the monomers in the 25 wt% solution are less hydrated. This is possibly due to the smaller number of water molecules available per monomer in the concentrated 25 wt% solution reducing the number of contacts in comparison with a semidilute solution.

Changes in the $\nu_{as}(CH_2)$ band in the 25 wt% PNIPAM solution in $D_2O$ (Figure 9c and d, blue triangles) are less pronounced than the $\nu_{as}(CH_3)$ mode. They are related to the hydrophobic hydration of the backbone. At atmospheric pressure, the peak frequency shifts abruptly to a lower frequency at $T_{cp}$, above which it remains constant. At 130 MPa the decrease in frequency at $T_{cp}$ is smaller. It can be concluded that the dehydration of the backbone at $T_{cp}$ is weaker at high pressure.

We now turn to the 25 wt% PNIPAM solution in 80:20 v/v $D_2O/CD_3OD$. It was previously shown, that solvation of hydrophobic groups with an organic solvent does not lead to an increase in stretching frequency.[100] Thus, the shift of the frequencies of the asymmetric stretching bands of $CH_3$ and $CH_2$ in the PNIPAM solution in $D_2O/CD_3OD$ to lower frequencies than in the purely aqueous PNIPAM solution in the one-phase region can be attributed to a weaker hydration of the

hydrophobic groups in the solvent mixture than in neat $D_2O$. This is the case both at atmospheric and at high pressure. At atmospheric pressure, it is in line with the partial replacement of water by methanol on the hydrophobic groups of PNIPAM. It is in agreement with the preferential adsorption of methanol inferred from the QENS data (Figure 7a), and with recent molecular dynamics simulations on aqueous PNIPAM solutions including ethanol as a cosolvent.[101] At high pressure, however, nearly all methanol molecules are expelled from the chains (Figure 7b). Therefore, the presence of methanol in the solution weakens the total solvation of hydrophobic groups in the one-phase region at high pressure.

At atmospheric pressure, the frequencies of both vibrational modes decrease abruptly at $T_{cp}$ and remain constant above. In contrast, at 200 MPa, the decrease is less pronounced and gradual in all cases. Thus, for PNIPAM dissolved in both $D_2O$ and $D_2O/CD_3OD$, the decrease of the stretching frequencies of the asymmetric stretching modes of $CH_2$ and $CH_3$ may be attributed to the release of water molecules from the hydrophobic groups at $T_{cp}$, as the phase separation takes place. It occurs abruptly at atmospheric pressure and gradually at 200 MPa.

The frequencies of the $\nu_{as}(CH_2)$ and the $\nu_{as}(CH_3)$ vibrations in the 25 wt% PNIPAM solution in $D_2O/CD_3OD$ in the one-phase region are lower at atmospheric pressure than at 200 MPa. Thus, the hydrophobic groups are more strongly hydrated at 200 MPa than at 0.1 MPa. Since $f_h$ (Figure 6c and d) is generally smaller at 200 MPa than at 0.1 MPa close to the respective cloud points in the one-phase region, it can be concluded that the stronger hydrophobic hydration at 200 MPa must be compensated by a weaker hydrophilic hydration. On the other hand, the larger value of $\tau_h$ at 200 MPa than at 0.1 MPa in the same temperature range (Figure 7c and d) points to stronger binding of water molecules at 200 MPa. Specific water-methanol interactions on the chains or the

presence of a second hydration shell around adsorbed methanol molecules at 0.1 MPa contributing to $f_h$ may explain the difference. Further studies are needed to clarify this issue.

## Conclusions

We have investigated the dynamics of bulk and hydration water in a 25 wt% PNIPAM solution in 80:20 v/v $H_2O/CD_3OD$ at variable temperature and pressure using quasi-elastic neutron scattering and Raman spectroscopy. The one phase region is hugely expanded along the pressure axis with the coexistence line having a maximum near 200 MPa. The experimental results shed new light on the molecular mechanism and the importance of hydration for the reversal of co-non-solvency at high pressure. At atmospheric pressure, the susceptibility spectra provide evidence of polymer bound water, part of which is released during the LCST transition. Simultaneously, the elastic line strength increases abruptly which is consistent with a coil to globule transition. At a pressure of 200 MPa, the polymer chains stay more hydrated over the whole temperature range. The release of polymer bound water is gradual across the demixing transition, while there is a pronounced increase in the elastic line.

The diffusive properties of water in the bulk solvent phase show that at atmospheric pressure deep in the one-phase region the solvent phase is enriched with water, implying that methanol is preferentially adsorbed on the chains. With temperature increasing towards $T_{cp}$, the effective solvent composition approaches the nominal 80:20 v/v ratio, i.e., preferential adsorption is diminished. At 200 MPa, the composition of the bulk solvent phase is 80:20 v/v deep in the one-phase region, but approaches a 70:30 v/v ratio near $T_{cp}$. This demonstrates that, at high pressure, the solvent phase is enriched with methanol near $T_{cp}$, which in turn means that, under these conditions, water is preferentially adsorbed on the chains, leading to the breakdown of co-non-

solvency at high pressure. The relaxation time of the hydration water in the one-phase region, i.e., of water that is bound to the polymer, is larger at 200 MPa than at 0.1 MPa, which is in part due to a weakening effect of adsorbed methanol molecules on the binding strength of water with PNIPAM at atmospheric pressure.

Complementary Raman spectroscopy measurements probe the interaction between the solvent molecules and the hydrophobic groups of PNIPAM. At both pressures in the one-phase region, the hydration of the hydrophobic groups of PNIPAM in the presence of methanol is weaker than in a purely aqueous PNIPAM solution. This observation points to a replacement of water by methanol at the hydrophobic groups at atmospheric pressure and an overall weaker solvent adsorption by the hydrophobic groups at high pressure. In both solutions at high pressure, the hydrophobic groups are more strongly hydrated than at atmospheric pressure. As phase separation takes place, water molecules are released from the hydrophobic groups in all cases.

The wide range of timescales accessed by QENS in combination with variations in pressure makes possible the simultaneous investigation of the dynamics of hydration and bulk water. Release and adsorption of solutes by the polymer chains correlate with a change in effective solvent composition as evidenced by the diffusive properties of water in the bulk solvent mixture. Pressure modifies the hydrophobic interaction that plays a crucial role for the phase behavior. These effects may be central to the largely expanded one phase region along the pressure axis in the phase diagram with methanol as a cosolvent compared to neat water. The wide ranges in frequency and temperature at atmospheric and high pressure allow to distinguish the relaxation of hydration and bulk water. The measured susceptibility spectra complement previous measurements on the chain conformation and the entropic and enthalpic interactions between the

chains and the solvent mixture. They offer a sensitive test for molecular dynamics simulations and theoretical studies.

## ASSOCIATED CONTENT

**Supporting Information**. The following files are available free of charge. Coherent and incoherent scattering contributions to QENS. Cloud point determination by turbidimetry. Water dynamics in water/methanol mixtures. Effect of pressure on dynamic properties around the phase transition temperatures. Determination of the effective solvent composition adsorbed on PNIPAM. Deconvolution of Raman spectra. (PDF)

## AUTHOR INFORMATION

Corresponding Author

*Christine M. Papadakis, papadakis@tum.de.

*Alfons Schulte, alfons.schulte@ucf.edu.

### Author Contributions

The manuscript was written through contributions of all authors. All authors have given approval to the final version of the manuscript.

### Funding Sources

Funding by Deutsche Forschungsgemeinschaft (DFG) is gratefully acknowledged (PA 771/22-1). A. S. acknowledges support by an August-Wilhelm Scheer visiting professorship at TU Munich and sabbatical support from the University of Central Florida.

### Notes

The authors declare no competing financial interest.

ACKNOWLEDGMENT

This work is based upon experiments performed at the TOFTOF instrument operated by Technische Universität München at the Heinz Maier-Leibnitz Zentrum (MLZ), Garching, Germany. MLZ is acknowledged for allocating beam time and for excellent equipment. We thank A. Deyerling, Technical University of Munich, for turbidimetry measurements and H. Meier, MLZ, for technical assistance during the QENS experiment.

REFERENCES

(1) Strickley, R. G. Solubilizing Excipients in Oral and Injectable Formulations. *Pharm. Res.* **2004**, *21*, 201-230.

(2) Seedher, N.; Kanojia, M. Co-Solvent Solubilization of Some Poorly-Soluble Antidiabetic Drugs. *Pharm. Dev. Technol.* **2009**, *14*, 185-192.

(3) Canchi, D. R.; García, A. E. Cosolvent Effects on Protein Stability. *Annu. Rev. Phys. Chem.* **2013**, *64*, 273-293

(4) van der Vegt, N. F. A.; Nayar, D. The Hydrophobic Effect and the Role of Cosolvents. *J. Phys. Chem. B* **2017**, *121*, 9986-9998.

(5) Krieg, E.; Shih, W. M. Selective Nascent Polymer Catch-and-Release Enables Scalable Isolation of Multi-Kilobase Single-Stranded DNA. *Angew. Chem. Int. Ed.* **2018**, *57*, 714-718.

(6) Hirotsu, S.; Hirokawa, Y.; Tanaka, T. Volume-Phase Transitions of Ionized *N*-isopropylacrylamide Gels. *J. Chem. Phys.* **1987**, *87*, 1392-1395.

(7) Winnik, F. M.; Ringsdorf, H.; Venzmer, J. Methanol-Water as a Co-nonsolvent System for Poly(*N*-isopropylacrylamide). *Macromolecules* **1990**, *23*, 2415-2416.

(8) Mochizuki, K. On-Off of Co-non-solvency for Poly(*N*-vinylcaprolactam) in Alcohol-Water Mixtures: A Molecular Dynamics Study. *J. Phys. Chem. B* **2020**, 9951-9957.

(9) Mukherji, D.; Marques, C. M.; Kremer, K. Smart Responsive Polymers: Fundamentals and Design Principles. *Annu. Rev. Condens. Matter Phys.* **2020**, *11*, 271-299.

(10) Halperin, A.; Kröger, M.; Winnik, F. M. Poly(*N*-isopropylacrylamide) Phase Diagrams: Fifty Years of Research. *Angew. Chem. Int. Ed.* **2015**, *54*, 15342-15367

(11) Abott, L. J.; Tucker, A. K.; Stevens, M. J. Single Chain Structure of a Poly(*N*-isopropylacrylamide) Surfactant in Water. *J. Phys. Chem. B* **2015**, *119*, 3837-3845

(12) Zhang, G.; Wu, C. The Water/Methanol Complexation Induced Reentrant Coil-to-Globule-to-Coil Transition of Individual Homopolymer Chains in Extremely Dilute Solution. *J. Am. Chem. Soc.* **2001**, *123*, 1376-1380.

(13) Wang, F.; Shi, Y.; Luo, S.; Chen, Y.; Zhao, J. Conformational Transition of Poly(*N*-isopropylacrylamide) Single Chains in its Cononsolvency Process: A Study by Fluorescence Correlation Spectroscopy and Scaling Analysis. *Macromolecules* **2012**, *45*, 9196-9204.

(14) Scherzinger, C.; Schwarz, A.; Bardow, A.; Leonhard, K.; Richtering, W. Cononsolvency of Poly-N-isopropylacrylamide (PNIPAM): Microgels versus Linear Chains and Macrogels. Curr. Opin. Colloid Interface Sci. 2014, 19, 84-94

(15) Osaka, N.; Shibayama, M.; Pressure Effects on Cononsolvency Behavior of Poly(*N*-isopropylacrylamide) in Water/DMSO Mixed Solvents. *Macromolecules* **2012**, *45*, 2171-2174.

(16) Ebeling, B.; Eggers, S.; Hendrich, N.; Nitschke, A.; Vana, P. Flipping the Pressure- and Temperature-Dependent Cloud-Point Behavior in the Cononsolvency System of Poly(*N*-isopropylacrylamide) in Water and Ethanol. *Macromolecules* **2014**, *47*, 1462-1469.

(17) Tanaka, F.; Koga, T.; Kaneda, I.; Winnik, F. M. Hydration, Phase Separation and Nonlinear Rheology of Temperature-Sensitive Water-Soluble Polymers. *J. Phys.: Condens. Matter* **2011**, *23*, 184105.

(18) Deshmukh, S. A.; Sankaranarayanan, S. K. R. S.; Suthar, K.; Mancini, D. C. Role of Solvation Dynamics and Local Ordering of Water in Inducing Conformational Transitions in Poly(*N*-isopropylacrylamide) Oligomers through the LCST. *J. Phys. Chem. B* **2012**, *116*, 2651-2663.

(19) Zuo, T.; Ma, C.; Jiao, G.; Han, Z.; Xiao, S.; Liang, H.; Hong, L.; Bowron, D.; Soper, A.; Han, C. C.; Cheng, H. Water/Cosolvent Attraction Induced Phase Separation: A Molecular Picture of Cononsolvency. *Macromolecules* **2019**, *52*, 457-464.

(20) Maeda, Y.; Higuchi, T.; Ikeda, I. Change in Hydration State During the Coil-Globule Transition of Aqueous Solutions of Poly(*N*-isopropylacrylamide) as Evidenced by FTIR Spectroscopy. *Langmuir* **2000**, *16*, 7503-7509.

(21) Abott, L. J.; Tucker, A. K.; Stevens, M. J. Single Chain Structure of a Poly(*N*-isopropylacrylamide) Surfactant in Water. *J. Phys. Chem. B* **2015**, *119*, 3837-3845.

(22) Futscher, M. H.; Philipp, M.; Müller-Buschbaum, P.; Schulte, A. The Role of Backbone Hydration of Poly(*N*-isopropylacrylamide) Across the Volume Phase Transition Compared to its Monomer. *Sci. Rep.* **2017**, *7*, 17012.

(23) Okada, Y.; Tanaka, F. Cooperative Hydration, Chain Collapse, and Flat LCST Behavior in Aqueous Poly(*N*-isopropylacrylamide) Solutions. *Macromolecules* **2005**, *38*, 4465-4471.

(24) Shiraga, K.; Naito, H.; Suzuki, T.; Kondo, N.; Ogawa, Y. Hydration and Hydrogen Bond Network of Water during the Coil-to-Globule Transition of Poly(*N*-isopropylacrylamide) Aqueous Solution at Cloud Point Temperature. *J. Phys. Chem. B* **2015**, *119*, 5576-5587.

(25) Osaka, N.; Shibayama, M.; Kikuchi, T.; Yamamuro, O. Quasi-Elastic Neutron Scattering Study on Water and Polymer Dynamics in Thermo/Pressure Sensitive Polymer Solutions. *J. Phys. Chem. B* **2009**, *113*, 12870-12876.

(26) Philipp, M.; Kyriakos, K.; Silvi, L.; Lohstroh, W.; Petry, W.; Krüger, J. K.; Papadakis, C. M.; Müller-Buschbaum, P. From Molecular Dehydration to Excess Volumes of Phase-Separating PNIPAM Solutions. *J. Phys. Chem. B* **2014**, *118*, 4253-4260.

(27) Füllbrandt, M.; Ermilova, E.; Asadujjaman, A.; Hölzel, R.; Bier, F. F.; von Klitzing, R.; Schönhals, A. Dynamics of Linear Poly(*N*-isopropylacrylamide) in Water Around the Phase Transition Investigated by Dielectric Relaxation Spectroscopy. *J. Phys. Chem. B* **2014**, *118*, 3750-3759.

(28) Cho, E. C.; Lee, J.; Cho, K. Role of Bound Water and Hydrophobic Interaction in Phase Transition of Poly(*N*-isopropylacrylamide) Aqueous Solution. *Macromolecules* **2003**, *36*, 9929-9934.

(29) Ono, Y.; Shikata, T. Contrary Hydration Behavior of *N*-isopropylacrylamide to its Polymer, P(NIPAm), with a Lower Critical Solution Temperature. *J. Phys. Chem. B* **2007**, *111*, 1511-1513.

(30) Kyriakos, K.; Philipp, M.; Silvi, L.; Lohstroh, W.; Petry, W.; Müller-Buschbaum, P.; Papadakis, C. M. Solvent Dynamics in Solutions of PNIPAM in Water/Methanol Mixtures – A Quasi-Elastic Neutron Scattering Study. *J. Phys. Chem. B* **2016**, *120*, 4679-4688.

(31) Yang, M.; Zhao, K. Cononsolvency of Poly(N-isopropylacrylamide) in Methanol Aqueous Solution – Insight by Dielectric Spectroscopy. *J. Polym. Sci. B Polym. Phys*. **2017**, *55*, 1227-1234

(32) Tanaka, F.; Koga, T.; Kojima, H.; Xue, N.; Winnik, F. M. Preferential Adsorption and Co-nonsolvency of Thermoresponsive Polymers in Mixed Solvents of Water/Methanol. *Macromolecules* **2011**, *44*, 2978-2989.

(33) Mukherji, D.; Marques, C. M.; Kremer, K. Polymer Collapse in Miscible Good Solvents is a Generic Phenomenon Driven by Preferential Adsorption. *Nat. Commun.* **2014**, *5*, 4882.

(34) Rodríguez-Ropero, F.; Hajari, T.; van der Vegt, N. F. A. Mechanism of Polymer Collapse in Miscible Good Solvents. *J. Phys. Chem. B* **2015**, *119*, 15780-15788.

(35) Pica, A.; Graziano, G. An Alternative Explanation of the Cononsolvency of Poly(*N*-isopropylacrylamide) in Water-Methanol Solutions. *Phys. Chem. Chem. Phys.* **2016**, *18*, 25601-25608.

(36) Tavagnacco, L.; Zaccarelli, E.; Chiessi, E. Molecular Description of the Coil-to-Globule Transition of Poly(*N*-isopropylacrylamide) in Water/Ethanol Mixture at Low Alcohol Concentration. *J. Mol. Liq.* **2020**, *297*, 111928.

(37) Zhang, G.; Wu, C. Reentrant Coil-to-Globule-to-Coil Transition of a Single Linear Homopolymer Chain in a Water/Methanol Mixture. *Phys. Rev. Lett.* **2001**, *86*, 822-825.

(38) Hao, J.; Cheng, H.; Butler, P.; Zhang, L.; Han, C. C. Origin of Cononsolvency, Based on the Structure of Tetrahydrofuran-Water Mixture. *J. Chem. Phys.* **2010**, *132*, 154902.

(39) Osaka, N.; Shibayama, M. Pressure Effects on Cononsolvency Behavior of Poly(*N*-isopropylacrylamide) in Water/DMSO Mixed Solvents. *Macromolecules* **2012**, *45*, 2171-2174.

(40) Ebeling, B.; Eggers, S.; Hendrich, N.; Nitschke, A.; Vana, P. Flipping the Pressure- and Temperature-Dependent Cloud-Point Behavior in the Cononsolvency System of Poly(*N*-isopropylacrylamide) in Water and Ethanol. *Macromolecules* **2014**, *47*, 1462-1469.

(41) Shibayama, M.; Isono, K.; Okabe, S.; Karino, T.; Nagao, M. SANS Study on Pressure-Induced Phase Separation of Poly(*N*-isopropylacrylamide) Aqueous Solutions and Gels. *Macromolecules* **2004**, *37*, 2909-2918.

(42) Kunugi, S.; Yamazaki, Y.; Takano, K.; Tanaka, N.; Akashi, M. Effects of Ionic Additives and Ionic Comonomers on the Temperature and Pressure Responsive Behavior of Thermoresponsive Polymers in Aqueous Solutions. *Langmuir* **1999**, *15*, 4056-4061.

(43) Niebuur, B.-J.; Chiappisi, L.; Zhang, X.; Jung, F.; Schulte, A.; Papadakis, C. M. Formation and Growth of Mesoglobules in Aqueous Poly(*N*-isopropylacrylamide) Solutions Revealed with Kinetic Small-Angle Neutron Scattering and Fast Pressure Jumps. *ACS Macro Lett.* **2018**, *7*, 1155-1160.

(44) Ghosh, T.; García, A. E.; Garde, S. Molecular Dynamics Simulations of Pressure Effects on Hydrophobic Interactions. *J. Am. Chem. Soc.* **2001**, *123*, 10997-11003.

(45) Ghosh, T.; García, A. E.; Garde, S. Enthalpy and Entropy Contributions to the Pressure Dependence of Hydrophobic Interactions. *J. Chem. Phys.* **2002**, *116*, 2480-2486.

(46) Rick, S. W. Free Energy, Entropy and Heat Capacity of the Hydrophobic Interaction as a Function of Pressure. *J. Phys. Chem. B* **2000**, *104*, 6884-6888.

(47) Raúl Grigera, J.; McCarthy, A. N. The Behavior of the Hydrophobic Effect under Pressure and Protein Denaturation. *Biophys. J.* **2010**, *98*, 1626-1631.

(48) Dadarlat, V. M.; Post, C. B. Decomposition of Protein Experimental Compressibility into Intrinsic and Hydration Shell Contributions. *Biophys. J.* **2006**, *91*, 4544-4554.

(49) Smolin, N.; Winter, R. A Molecular Dynamics Simulation of Snase and its Hydration shell at High Temperature and High Pressure. *Biochim. Biophys. Acta* **2006**, *1764*, 522-534.

(50) Paschek, D.; Hempel, S.; García, A. E. Computing the Stability Diagram of the Trp-Cage Miniprotein. *Proc. Natl. Acad. Sci. U.S.A.* **2008**, *105*, 17754-17759.

(51) Sarupria, S.; Garde, S. Quantifying Water Density Fluctuations and Compressibility of Hydration Shells of Hydrophobic Solutes and Proteins. *Phys. Rev. Lett.* **2009**, *103*, 037803.

(52) Meersman, F.; Wang, J.; Wu, Y.; Heremans, K. Pressure Effect on the Hydration Properties of Poly(*N*-isopropylacrylamide) in Aqueous Solution Studied by FTIR Spectroscopy. *Macromolecules* **2005**, *38*, 8923-8928.

(53) Niebuur, B.-J.; Claude, K.-L.; Pinzek, S.; Cariker, C.; Raftopoulos, K. N.; Pipich, V.; Appavou, M.-S.; Schulte, A.; Papadakis, C. M. Pressure-Dependence of Poly(*N*-isopropylacrylamide) Mesoglobule Formation in Aqueous Solution. *ACS Macro Lett.* **2017**, *6*, 1180-1185.

(54) Tavagnacco, L.; Chiessi, E.; Zaccarelli, E. Molecular Insights on Poly(*N*-isopropylacrylamide) Coil-to-Globule Transition Induced by Pressure. arXiv:2008.09324

(55) Niebuur, B.-J.; Chiappisi, L.; Jung, F.; Zhang, X.; Schulte, A.; Papadakis, C. M. Kinetics of Mesoglobule Formation and Growth in Aqueous Poly(*N*-isopropylacrylamide) Solutions. Pressure Jumps at Low and at High Pressure. *Macromolecules* **2019**, *52*, 6416-6427.

(56) Niebuur, B.-J.; Lohstroh, W.; Appavou, M.-S.; Schulte, A.; Papadakis, C. M. Water Dynamics in a Concentrated Poly(*N*-isopropylacrylamide) Solution and Variable Pressure. *Macromolecules* **2019**, *52*, 1942-1954.

(57) de Oliveira, T. E.; Netz, P. A.; Mukherji, D.; Kremer, K. Why Does High Pressure Destroy Co-Non-Solvency of PNIPAm in Aqueous Methanol? *Soft Matter* **2015**, *11*, 8599-8604.

(58) Pica, A.; Graziano, G. Hydrostatic Pressure Effect on PNIPAM Cononsolvency in Water-Methanol Solutions. *Biophys. Chem.* **2017**, *231*, 34-38.

(59) Hofmann, C. H.; Grobelny, S.; Erlkamp, M.; Winter, R.; Richtering, W. Influence of High-Pressure on Cononsolvency of Poly(*N*-isopropylacrylamide) Nanogels in Water/Methanol Mixtures. *Polymer* **2014**, *55*, 2000-2007.

(60) Yong, H.; Merlitz, H.; Fery, A.; Sommer, J-.U. Polymer Brushes and Gels in Competing Solvents: The Role of Different Interactions and Quantitative Predictions for Poly(*N*-isopropylacrylamide) in Alcohol-Water Mixtures. *Macromolecules* **2020**, *53*, 2323-2335.

(61) Niebuur, B.-J.; Ko, C.-H.; Zhang, X.; Claude, K.-L.; Chiappisi, L.; Schulte, A.; Papadakis, C. M. Pressure Dependence of the Cononsolvency Effect in Aqueous Poly(*N*-isopropylacrylamide) Solutions: A SANS Study. *Macromolecules* **2020**, *53*, 3946-3955.

(62) Unruh, T.; Neuhaus, J.; Petry, W. The High-Resolution Time-of-Flight Spectrometer TOFTOF. *Nucl. Instrum. Methods Phys. Res. A* **2007**, *580*, 1414-1422.

(63) Heinz Maier-Leibnitz Zentrum et al. TOFTOF: Cold Neutron Time-of-Flight Spectrometer. *JLSRF* 2015, 1, A15.

(64) Appavou, M.-S.; Busch, S.; Doster, W.; Gaspar, A.; Unruh, T. The Influence of 2 kbar Pressure on the Global and Internal Dynamics of Human Hemoglobin Observed by Quasielastic Neutron Scattering. *Eur. Biophys. J.* **2011**, *40*, 705-714.

(65) Arnold, O.; Bilheux, J. C.; Borreguero, J. M.; Buts, A.; Campbell, S. I.; Chapon, L.; Doucet, M.; Draper, N.; Ferraz Leal, R.; Gigg, M. A.; Lynch, V. E.; Markvardsen, A.; Mikkelson, D. J.; Mikkelson, R. L.; Miller, R.; Palmen, K.; Parker, P.; Passos, G.; Perring, T. G.; Peterson, P. F.; Ren, S.; Reuter, M. A.; Savici, A. T.; Taylor, J. W.; Taylor, R. J.; Tolchenov, R.; Zhou, W.; Zikovsky, J. Mantid – Data Analysis and Visualization Package for Neutron Scattering and μ SR Experiments. *Nucl. Instr. Meth. Phys. Res. B* **2014**, *764*, 156-166.

(66) Rolston, J. H.; Gale, K. L. Fractionation of Deuterium and Protium Between Water and Methanol. *J. Phys. Chem.* **1984**, *88*, 4394-4397.

(67) Doster, W.; Cusack, S.; Petry, W. Dynamic Instability of Liquid-like Motions in a Globular Protein Observed by Inelastic Neutron Scattering. *Phys. Rev. Lett.* **1990**, *65*, 1080-1083.

(68) Bizzarri, A. R.; Cannistraro, S. Molecular Dynamics of Water at the Protein-Solvent Interface. *J. Phys. Chem. B* **2002**, *106*, 6617-6633.

(69) Arbe, A.; Malo de Molina, P.; Alvarez, F.; Brick, B.; Colmenero, J. Dielectric Susceptibilities of Liquid Water: Microscopic Insights from Coherent and Incoherent Neutron Scattering. *Phys. Rev. Lett.* **2016**, *117*, 185501.

(70) Perticaroli, S.; Ehlers, G.; Stanly, C. B.; Mamontov, E.; O'Neill, H.; Zhang, Q.; Cheng, X.; Myles, D. A. A.; Katsaras, J.; Nickels, J. D. Description of Hydration Water in Protein (Green Fluorescent Protein) Solution. *J. Am. Chem. Soc.* **2017**, *139*, 1098-1105.

(71) Roh, J. H.; Curtis, J. E.; Azzam, S.; Novikov, V. N.; Peral, I.; Chowdhuri, Z.; Gregory, R. B.; Sokolov, A. P. Influence of Hydration on the Dynamics of Lysozyme. *Biophys. J.* **2006**, *91*, 2573-2588.

(72) Bergman, R. General Susceptibility Functions for Relaxations in Disordered Systems. *J. Appl. Phys.* **2000**, *88*, 1356-1365.

(73) Derlacki, Z. J.; Easteal, A. J.; Edge, A. V. J.; Woolf, L. A.; Roksandic, Z. Diffusion Coefficients of Methanol and Water and the Mutual Diffusion Coefficient in Methanol-Water Solutions at 278 and 298 K. *J. Phys. Chem.* **1985**, *89*, 5318-5322.

(74) Fåk, B.; Dorner, B. Phonon Line Shapes and Excitation Energies. *Physica B* **1997**, *234-236*, 1107-1108.

(75) Ohmine, I. Liquid Water Dynamics: Collective Motions, Fluctuations, and Relaxation. *J. Phys. Chem.* **1995**, *99*, 6767-6776.

(76) Walrafen, G. W.; Chu, Y. C. Linearity Between Structural Correlation Length and Correlated-Proton Raman Intensity from Amorphous Ice and Supercooled Water up to Dense Supercritical Steam. *J. Phys. Chem.* **1995**, *99*, 11225-11229.

(77) Wan, Q.; Spanu, L.; Galli, G. A.; Gygi, F. Raman Spectra of Liquid Water from Ab Initio Molecular Dynamics: Vibrational Signatures of Charge Fluctuations in the Hydrogen Bond Network. *J. Chem. Theory Comput.* **2013**, *9*, 4124-4130.

(78) Qvist, J.; Schober, H.; Halle, B. Structural Dynamics of Supercooled Water from Quasielastic Neutron Scattering and Molecular Simulations. *J. Chem. Phys.* **2011**, *134*, 144508.

(79) Teixeira, J.; Bellissent-Funel, M.-C.; Chen, S. H.; Dianoux, A. J. Experimental Determination of the Nature of Diffusive Motions of Water Molecules at Low Temperatures. *Phys. Rev. A* **1985**, *31*, 1913-1917.

(80) Nakada, M.; Maruyama, K.; Yamamuro, O.; Misawa, M. Quasielastic Neutron Scattering Investigation of Motion of Water Molecules in *n*-Propyl Alcohol-Water Mixture. *J. Chem. Phys.* **2009**, *130*, 074503.

(81) Alam, M. K.; Callis, J. B. Elucidation of Species in Alcohol-Water Mixtures Using Near-IR Spectroscopy and Multivariate Statistics. *Anal. Chem.* **1994**, *66*, 2293-2301.

(82) Corsaro, C.; Spooren, J.; Branca, C.; Leone, N.; Broccio, M.; Kim, C.; Chen, S.-H.; Stanley, H. E.; Mallamace, F. Clustering Dynamics in Water/Methanol Mixtures: A Nuclear Magnetic Resonance Study at 205 K < $T$ < 295 K. *J. Phys. Chem. B* **2008**, *112*, 10449-10454.

(83) Soper, A. K.; Finney, J. L. Hydration of Methanol in Aqueous Solution. *Phys. Rev. Lett.* **1993**, *71*, 4346-4349.

(84) Laaksonen, A.; Kusalik, P. G.; Svishchev, I. M. *J. Phys. Chem. A* **1997**, *101*, 5910-5918.

(85) Li, F.; Cui, Q.; He, Z.; Cui, T.; Zhang, J.; Zhou, Q.; Zou, G. High Pressure-Temperature Brillouin Study of Liquid Water: Evidence of the Structural Transition from Low-Density Water to High-Density Water. *J. Chem. Phys.* **2005**, *123*, 174511.

(86) Del Corro, E.; Cáceres, M.; Taravillo, M.; Núñez, J.; Baonza, V. G. Raman Spectroscopy of Aqueous Methanol Solutions under Pressure. *High Press. Res.* **2006**, *26*, 407-410.

(87) Hsieh, W.-P.; Chien, Y.-H. High Pressure Raman Spectroscopy of $H_2O$-$CH_3OH$ Mixtures. *Sci. Rep.* **2015**, *5*, 8532.

(88) Ramakrishnan, G.; González-Jiménez, M.; Lapthorn, A. J.; Wynne, K. Spectrum of Slow and Super-Slow (Picosecond to Nanosecond) Water Dynamics around Organic and Biological Solutes. *J. Phys. Chem. Lett.* **2017**, *8*, 2964-2970.

(89) Doster, W.; Gebhardt, R. High Pressure-Unfolding of Myoglobin Studied by Dynamic Neutron Scattering. *Chem. Phys.* **2003**, *292*, 383-387.

(90) Rubio Retama, J.; Frick, B.; Seydel, T.; Stamm, M.; Fernandez Barbero, A.; López Cabarcos, E. Polymer Chain Dynamics of Core-Shell Thermosensitive Microgels. *Macromolecules* **2008**, *41*, 4739-4745.

(91) Laage, D.; Stirnemann, G.; Hynes, J. T. Why Water Reorientation Slows Without Iceberg Formation around Hydrophobic Solutes. *J. Phys. Chem. B* **2009**, *113*, 2428-2435.

(92) Sterpone, F.; Stirnemann, G.; Hynes, J. T.; Laage, D. Water Hydrogen-Bond Dynamics around Amino Acids: The Key Role of Hydrophilic Hydrogen-Bond Acceptor Groups. *J. Phys. Chem. B* **2010**, *114*, 2083-2089.

(93) Laage, D.; Stirnemann, G.; Sterpone, F.; Rey, R.; Hynes, J. T. Reorientation and Allied Dynamics in Water and Aqueous Solutions. *Annu. Rev. Phys. Chem.* **2011**, *62*, 395-416.

(94) Sun, B.; Lin, Y.; Wu, P. Structure Analysis of Poly(*N*-isopropylacrylamide) Using Near-Infrared Spectroscopy and Generalized Two-Dimensional Correlation Infrared Spectroscopy. *Appl. Spectrosc.* **2007**, *61*, 765-771.

(95) Sun, B.; Lin, Y.; Wu, P.; Siesler, H.W. A FTIR and 2D-IR Spectroscopic Study on the Microdynamics Phase Separation Mechanism of the Poly(*N*-isopropylacrylamide) Aqueous Solution. *Macromolecules* **2008**, *41*, 1512-1520.

(96) Hobza, P.; Havlas, Z. Blue-Shifting Hydrogen Bonds. *Chem. Rev.* **2000**, *100*, 4253-4264.

(97) Scheiner, S.; Kar, T. Red- Versus Blue-Shifting Hydrogen Bonds: Are There Fundamental Distinctions? *J. Phys. Chem. A* **2002**, *106*, 1784-1789.

(98) Kar, T.; Scheiner, S. Comparison of Cooperativity in CH···O and OH···O Hydrogen Bonds. *J. Phys. Chem. A* **2004**, *108*, 9161-9168.

(99) Joseph, J.; Jemmis, E.D. Red-, Blue-, or No-Shift in Hydrogen Bonds: A Unified Explanation. *J. Am. Chem. Soc.* **2007**, *129*, 4620-4632.

(100) Yamauchi, H.; Maeda, Y. LCST and UCST Behavior of Poly(*N*-isopropylacrylamide) in DMSO/Water Mixed Solvents Studied by IR and Micro-Raman Spectroscopy. *J. Phys. Chem. B* **2007**, *111*, 12964-12968.

(101) Tavagnacco, L.; Zaccarelli, E.; Chiessi, E. Molecular Description of the Coil-to-Globule Transition of Poly(*N*-isopropylacrylamide) in Water/Ethanol Mixture at Low Alcohol Concentration. *J. Mol. Liq.* **2020**, *297*, 111928.